Astronomy & Astrophysics manuscript no. April 10, 2002
(DOI: will be inserted by hand later)

Observations of the OH 18-cm lines in comets at Nançay:

The data base. Observations made from 1982 to 1999.

J. Crovisier, P. Colom, E. Gérard, D. Bockelée-Morvan, and G. Bourgois⋆

Observatoire de Paris-Meudon, F-92195 Meudon, France

Received / Accepted

Abstract. Since the apparition of comet Kohoutek 1973 XII, the 18-cm lines of the OH radical have been systematically observed in a number of comets with the Nançay radio telescope. Between 1973 and 1999, 52 comets have been successfully detected. This allowed an evaluation of the cometary water production rates and their evolution with time, as well as a study of several physical processes such as the excitation mechanisms of the OH radio lines, the expansion of cometary atmospheres, their anisotropy in relation with non-gravitational forces, and the Zeeman effect in relation with the cometary magnetic field. Part of these observations and their analysis have already been published. The bulk of the results are now organized in a data base. The present paper is a general presentation of the Nançay cometary data base and a more specific description of the observations of 53 cometary apparitions between 1982 and 1999. Comets observed before 1982 are only partly incorporated in the data base. Observations of comets since 2000 benefited from a major upgrade of the telescope; they will be presented in forthcoming publications.

Key words. comets – molecules – OH radical – radio lines – spectroscopy

1. Introduction

A new era in the study of comets began in 1973 with the observations of the 18-cm lines of the OH radical, first detected in comet Kohoutek 1973 XII[1] (Biraud et al. 1974; Turner 1974). This discovery initiated a long-term programme of observation at the Nançay radio telescope (Table 1).

The OH radical in cometary atmospheres comes from the photodissociation of water, the major constituent of cometary ices. The direct observation of cometary water from the ground is difficult and one usually has to rely on secondary products such as OH to assess the outgassing of comets and its evolution. The OH radical can be observed through its A–X electronic system in the near UV, which can be done from the ground under good observing conditions (e.g., A'Hearn et al. 1995), or from space with dedicated instruments (e.g., Feldman 1999). The vibrational bands of OH can also be observed in the infrared (either from space or from the ground), but this has only been possible in a few cases. Radio observations of the 18-cm lines of OH are quite different from UV or infrared spectroscopic observations. Radio lines are fully resolved and their Doppler profiles allow us to investigate the kinematic properties of the cometary atmosphere. This is hardly possible at other wavelengths. The radio telescope beam samples a large part of the coma, so that minimal extrapolations to the whole coma are required (in contrast to typical visible or UV spectroscopic observations, which sample only a very small fraction of the coma). Radio observations at 18-cm wavelength do not have visibility constraints such as solar elongation and are almost insensitive to weather conditions. However, because of the particularities of the excitation mechanism of the OH radical, which depends upon the heliocentric radial velocity (see Sect. 3), the observation of the 18-cm OH lines is only possible part of the time.

The purpose of the present paper is to describe the set of cometary observations made at Nançay in the 1982–1999 period, which began with the implementation of an efficient autocorrelator spectrometer and ended with a major upgrading of the telescope.

Send offprint requests to: J. Crovisier;
email: Jacques.Crovisier@obspm.fr

⋆ deceased

[1] The old-style designation is retained here for comets observed before 1995. Cross-references between old- and new-style designations are given in Table 1.

Table 1. The comets observed at Nançay up to 1999

comet a)	b)	c)	perihelion [yymmdd]	q [AU]	range of observations [yymmdd]	r range d) [AU]	e)	f)	g)	h)
1973 XII	1973f	C/1973 E1 Kohoutek	731228.43	0.142	731129–740215			N	D	
1975 IX	1975h	C/1975 N1 Kobayashi-Berger-Milon	750905.33	0.426	750826–750904			L	D	
1976 VI	1975n	C/1975 V1 West	760225.22	0.197	760324–760512			L	D	
1977 XI		2P/Encke	770817.01	0.341	770808–770911			J	-	
1977 XIV	1977m	C/1977 R1 Kohler	771110.57	0.991	771021–771130			L	D	
1978 VII	1978c	C/1978 C1 Bradfield	780317.69	0.437	780304–780316			L	D	
1978 XXI	1978f	C/1978 H1 Meier	781111.41	1.137	780531–781029			N	D	
1979 X	1979l	C/1979 Y1 Bradfield	791221.60	0.545	800127–800203			L	M	
1980 XI		2P/Encke	801206.58	0.340	800919–801229			J	M	
1980 XII	1980q	C/1980 V1 Meier	801209.65	1.520	801116–810218			L	D	
1980 XV	1980t	C/1980 Y1 Bradfield	801229.54	0.260	810103–810303			L	M	
1981 XIX	1981j	64P/Swift-Gehrels	811127.27	1.361	811031–811111			J	–	
1982 I	1980b	C/1980 E1 Bowell	820312.29	3.364	821127–821219	4.17–4.29	15	N	–	1
1982 IV	1982a	26P/Grigg-Skjellerup	820515.00	0.989	820507–820625	0.99–1.15	15	J	–	2
1982 VI	1982g	C/1982 M1 Austin	820824.73	0.648	820626–820905	0.65–1.33	38	L	D	3
1982 VII	1982e	6P/d'Arrest	820914.31	1.291	820708–820823	1.32–1.51	34	J	M	4
1982 VIII	1982f	67P/Churyumov-Gerasimenko	821112.10	1.306	821009–821025	1.32–1.37	7	J	M	5
1984 IV	1983n	27P/Crommelin	840220.17	0.735	840121–840320	0.73–0.92	35	H	M	6
1984 XIII	1984i	C/1984 N1 Austin	840912.14	0.291	840727–840811	0.29–0.55	14	L	D	7
1985 XIII	1984e	21P/Giacobini-Zinner	850905.21	1.028	850331–851120	1.03–2.20	117	J	D	8
1985 XVII	1985l	C/1985 R1 Hartley-Good	851209.12	0.695	850924–860113	0.70–1.54	93	L	D	9
1985 XIX	1985m	C/1985 T1 Thiele	851219.21	1.317	851027–851216	1.32–1.53	35	L	D	10
1986 III	1982i	1P/1982 U1 Halley	860209.45	0.587	850126–860729	0.59–5.04	408	H	D	11
1987 II	1986n	C/1986 V1 Sorrells	870309.65	1.721	870101–870214	1.62–2.44	10	L	D	12
1987 III	1987c	C/1987 B1 Nishikawa-Takamizawa-Tago	870317.29	0.872	870303–870312	0.88–0.91	10	L	D	13
1987 VII	1986l	C/1986 P1 Wilson	870420.78	1.200	860825–870622	1.24–3.42	116	L	D	14
1987 XXIX	1987s	C/1987 P1 Bradfield	871107.26	0.869	871001–871128	0.89–1.09	34	L	D	15
1988 I	1987d_1	C/1987 W1 Ichimura	880110.10	0.200	880103–880109	0.78–0.99	7	L	M	16
1988 V	1988a	C/1988 A1 Liller	880331.11	0.841	880317–880324	0.85–0.88	6	L	D	17
1988 XV	1988j	C/1988 P1 Machholz	880917.57	0.165	880912–881019	0.26–0.97	18	L	–	18
1989 X	1989o	23P/1989 N1 Brorsen-Metcalf	890911.94	0.479	890804–891031	0.48–1.17	61	H	D	19
1989 XIX	1989r	C/1989 Q1 Okazaki-Levy-Rudenko	891111.92	0.642	891003–891202	0.64–1.03	49	N	D	20
1989 XXII	1989a_1	C/1989 W1 Aarseth-Brewington	891227.89	0.301	891208–891230	0.30–0.63	19	L	D	21
1990 V	1989c_1	C/1989 X1 Austin	900409.97	0.350	900215–900615	0.35–1.52	100	N	D	22
1990 XX	1990c	C/1990 K1 Levy	901024.63	0.939	900616–900930	1.03–2.26	77	L	D	23
1992 III	1991g_1	C/1991 Y1 Zanotta-Brewington	920131.99	0.644	920109–920129	0.72–0.92	17	N	D	24
1992 VII	1992b	C/1992 B1 Bradfield	920319.54	0.500	920301–920312	1.02–1.14	10	L	–	25
1992 VIII	1991h_1	C/1991 X2 Mueller	920321.20	0.199	920305–920318	0.22–0.56	12	N	–	26
1992 XIX	1991a_1	C/1991 T2 Shoemaker-Levy	920723.75	0.829	920610–920722	0.84–1.16	38	L	D	27
1992 XXVIII	1992t	109P/1992 S2 Swift-Tuttle	921212.33	0.958	921015–930112	0.96–1.36	54	H	D	28
1993 III	1992x	24P/Schaumasse	930303.96	1.202	930121–930220	1.21–1.32	30	J	D	29
1994 V		2P/Encke	940209.47	0.331	940111–940303	0.34–0.77	36	J	M	30
1994 IX	1993p	C/1993 Q1 Mueller	940326.31	0.967	940120–940320	0.97–1.45	40	N	D	31
1994 XI	1993v	C/1993 Y1 McNaught-Russell	940331.09	0.868	940301–940420	0.96–1.02	25	L	D	32
1994 XV	1992r	8P/Tuttle	940625.29	0.998	940604–940616	1.01–1.05	12	H	M	33
1994 XXVI	1994o	141P/1994 P1 Machholz 2	940918.63	0.753	940908–940914	0.76–0.77	7	J	M	34
1994 XXX	1994l	19P/Borrelly	941101.49	1.365	940905–950118	1.39–1.62	51	J	D	35
		15P/Finlay	950505.04	1.036	950405–950422	1.04–1.12	17	J	–	36
		C/1995 Q1 Bradfield	950831.42	0.436	950824–950926	0.47–0.83	18	L	D	37
		73P/Schwassmann-Wachmann 3	950922.75	0.933	950830–951101	0.94–1.10	36	J	D	38
		122P/1995 S1 de Vico	951006.02	0.659	951001–951020	0.67–0.72	10	H	D	39
		45P/Honda-Mrkos-Pajdušáková	951225.93	0.532	951125–960120	0.53–0.81	37	J	M	40
		C/1996 B2 Hyakutake	960501.40	0.230	960301–960518	0.23–1.51	49	L	D	41
		22P/Kopff	960702.19	1.580	960409–960523	1.63–1.78	40	J	D	42
		C/1996 Q1 Tabur	961103.53	0.840	961002–961027	0.85–1.03	17	L	D	43
		C/1995 O1 Hale-Bopp	970401.13	0.914	950804–970921	0.91–7.04	329	L	D	44
		46P/Wirtanen	970314.14	1.064	970204–970509	1.07–1.30	40	J	–	45
		81P/Wild 2	970506.64	1.583	970121–970323	1.64–1.88	37	J	M	46
		2P/Encke	970523.60	0.331	970513–970522	0.33–0.43	9	J	–	47
		C/1998 J1 SOHO	980508.62	0.153	980601–980608	0.79–0.96	8	L	D	48
		C/1998 P1 Williams	981017.84	1.147	980918–981004	1.17–1.24	12	L	M	49
		21P/Giacobini-Zinner	981121.32	1.034	981020–981115	1.04–1.13	22	J	D	50
		C/1998 U5 LINEAR	981221.89	1.236	981124–981210	1.25–1.30	15	L	M	51
		C/1999 H1 Lee	990711.17	0.708	990508–990814	0.71–1.39	66	L	D	52
		C/1999 N2 Lynn	990723.05	0.761	990716–990719	0.76–0.77	4	L	D	53

a) old-style definitive designation; b) old-style provisional designation; c) new-style designation; d) lowest and highest heliocentric distances of the observations; e) number of observations in the data base; f) comet type; N: dynamically new, long-period comet; L: other long-period comet; H: Halley-type comet; J: Jupiter-family comet; g) –: no detection; M: marginal detection; D: clear detection; h) corresponding order number of the electronic tables and figures.

The resulting spectra are now organized in a data base where they can be accessed interactively. A dedicated software[2] (XCOM) allows us to display and process the spectra, and to retrieve physical parameters such as the OH production rates using model parameters specified by the user.

The scientific analysis of these data is beyond the scope of the present paper and is the subject of separate publications, present or future (Table 2):

- study of the excitation mechanisms of the OH radio lines (Biraud et al. 1974; Despois et al. 1981; Gérard 1990; Gérard et al. 1998; Colom et al. 1999);
- statistical analysis of the correlation between OH production rates and visual magnitudes (Despois et al. 1981; Bockelée-Morvan et al. 1981; Jorda 1995; Jorda et al. 1992, 1996);
- study of the long-term and short-term variability of the OH production rate in 1P/Halley (Gérard et al. 1987; Colom & Gérard 1988);
- analysis of the 18-cm line widths in relation with the expansion velocity of the atmosphere (Bockelée-Morvan & Gérard 1984; Bockelée-Morvan et al. 1990a);
- analysis of the 18-cm line profile in relation with anisotropic outgassing and non-gravitational forces (Bockelée-Morvan & Gérard 1984; Colom et al. 1990 and *in preparation*);
- study of the Zeeman effect and of its relation to the cometary magnetic field (Gérard 1985; Bockelée-Morvan et al. 1992; Gérard et al. 1993).

Section 2 describes the characteristics of the Nançay radio telescope and the observing procedures. Section 3 explains how OH production rates can be derived from the radio observations. Section 4 briefly recalls the 1973–1981 observations. Section 5 is a detailed description of the 1982–1999 observations while notes on individual comets are given in an Appendix. Section 6 discusses some statistical aspects of the data base. Section 7 concludes on the future of cometary observations at Nançay.

Most of the tables and figures of the present paper are only available in electronic form[3]. The Nançay spectra are public domain and may be requested from the authors. The data base itself and its companion software XCOM are not transportable and cannot be remotely accessed. They could be used, however, in collaboration with the authors.

[2] which is based upon the GILDAS software package (`http://iram.fr/GS/gildas.html`) developed at the Observatoire de Grenoble.

[3] via anonymous ftp to `cdsarc.u-strasbg.fr`, or to `http://cdsweb.u-strasbg.fr/Abstract.html` for the tables and to `http://www.edpsciences.orig` for the figures. Also independently available from `http://wwwusr.obspm.fr/~crovisie/basecom/referee.html`.

2. Observations

The Nançay radio telescope is a meridian instrument. It can observe sources at declination $\delta > -39°$ and can track them for about $\pm 1.1/\cos\delta$ hour. For observations at 18 cm wavelength, its RA $\times$ dec beam is $3.5' \times 19'$ at declinations lower than 30°. Its sensitivity for point sources is 0.9 K Jy^{-1} at $\delta \approx 0°$ and its variation with declination is given in Fig. 1 of Gérard et al. (1989). The system temperature was typically 45 K (at $\delta \approx 0°$) at the end of the observing period considered here.

Since 1982, all cometary observations are made using a 1024-channel autocorrelator split into 4×256–channel banks, allowing simultaneous observations of the OH 18-cm main lines at 1667 and 1665 MHz (except for occasional observations of the satellite lines at 1612 and 1721 MHz), and two polarizations (right- and left-circular polarizations, except for comets Bowell 1982 I and 6P/Churyumov-Gerasimenko 1982 VII which were observed in vertical and horizontal linear polarizations). In 1983, the Nançay radio telescope was closed for upgrading (installation of a new carriage house, of new computers and operating software). As a consequence, comets Sugano-Saigusa-Fujikawa 1983 V and IRAS-Araki-Alcock 1983 VII, which respectively passed at only 0.063 and 0.033 AU from the Earth, unfortunately could not be observed.

The autocorrelator is set to a 782 Hz channel separation, corresponding to 0.14 km s^{-1}. The effective resolution is 0.28 km s^{-1} after Hanning smoothing. A frequency-switching mode is used, with a frequency shift of 100 kHz. A $\sqrt{2}$ factor in the signal-to-noise ratio is gained after folding the spectra. The spectral coverage is about ± 8 km s^{-1}, which is enough for observing cometary spectra with a good determination of the baselines since the cometary line widths are typically 2 km s^{-1}. The comets are tracked in position and velocity using an ephemeris computed from the latest available orbital elements (which, except otherwise stated, are those distributed by the Central Bureau for Astronomical Telegrams). The occasional errors which resulted from inaccurate ephemeris are discussed in Sect. 5.

A check of the telescope performances and backend setup was done by frequently (usually every other day) observing the OH lines of the galactic source W12. The radial velocity scale was accurate within ± 0.02 km s^{-1}.

Interferences of external origin were very rare during the whole period 1973–1999 because most of the cometary observations were made in the main lines at 1665 and 1667 MHz. The protected radio astronomy band has a primary status over the whole range 1660.0 MHz–1670.0 MHz while the radial velocity of the nucleus with respect to the telescope never shifts the rest frequency by more than 0.5 MHz. Strong interferences of internal origin, however, were recorded in early 1982 which ruined the 1665 MHz observations (e.g., comet Bowell 1982 I) when a new receiver front-end was installed with improper local oscillator setting.

Table 2. Summary of papers published in refereed journals describing observations of comets at Nançay (see text for other publications)

Comet	reference
Kohoutek 1973 XII	Biraud et al. 1974
Kobayashi-Berger-Milon 1975 IX	Despois et al. 1981
West 1976 VI	Despois et al. 1981
P/Encke 1977 XI	Despois et al. 1981
Kohler 1977 XIV	Despois et al. 1981
Bradfield 1978 VII	Despois et al. 1981
Meier 1978 XXI	Bockelée-Morvan et al. 1981
Bradfield 1979 XX	Bockelée-Morvan et al. 1981
P/Encke 1980 XI	Bockelée-Morvan et al. 1981
Meier 1980 XII	Bockelée-Morvan et al. 1981
Bradfield 1980 XV	Bockelée-Morvan et al. 1981
Austin 1982 VI	Bockelée-Morvan & Gérard 1984, Gérard 1985, Bockelée-Morvan et al. 1990a
27P/Crommelin	Bockelée-Morvan et al. 1985
Austin 1984 XIII	Bockelée-Morvan et al. 1990a
21P/Giacobini-Zinner 1985 XIII	Gérard et al. 1988, Bockelée-Morvan et al. 1990a
Hartley-Good 1985 XVII	Bockelée-Morvan et al. 1990a
Thiele 1985 XIX	Bockelée-Morvan et al. 1990a
1P/Halley	Gérard et al. 1987, Colom & Gérard 1988, Gérard et al. 1989, Gérard 1990, Bockelée-Morvan et al. 1990a
Sorrells 1987 II	Bockelée-Morvan et al. 1990a
Wilson 1987 VII	Bockelée-Morvan et al. 1990a
Bradfield 1987 XXIX	Bockelée-Morvan et al. 1990a
Okazaki-Levy-Rudenko 1989 XIX	Crovisier et al. 1992
Zanotta-Brewington 1992 III	Bockelée-Morvan et al. 1994
Bradfield 1992 VII	Bockelée-Morvan et al. 1994
Mueller 1992 VIII	Bockelée-Morvan et al. 1994
Shoemaker -Levy 1992 XIX	Bockelée-Morvan et al. 1994
109P/Swift-Tuttle 1992 XXVIII	Bockelée-Morvan et al. 1994
24P/Schaumasse 1993 III	Bockelée-Morvan et al. 1994
73P/Schwassmann-Wachmann 3	Crovisier et al. 1996a
C/1996 B2 (Hyakutake)	Gérard et al. 1998
C/1995 O1 (Hale-Bopp)	Biver et al. 1996, 1997, Colom et al. 1999
C/1999 H1 (Lee)	Biver et al. 2000

3. OH production rates

The derivation of OH production rates from the observation of the OH 18-cm lines requires the knowledge of the excitation conditions of the OH radical and of its distribution within the coma; this has been debated for some time and some of the parameters necessary for the modelling of cometary OH are still poorly known. A brief discussion of the present situation and of the assumptions and parameters used in the present paper is now in order. The sets of parameters used in several previous studies and in the present work are summarized in Table 3.

The excitation through UV pumping and subsequent fluorescence leads to inversion (or anti-inversion) of the ground-state Λ-doublet of OH. Following pioneering works of Biraud et al. (1974) and Mies (1974), this process was modelled by Despois et al. (1981) and Schleicher & A'Hearn (1988), leading to an evaluation of the OH inversion as a function of heliocentric radial velocity similar – within details – in the two studies. The most notable divergence between the two model inversion curves is the small difference in the heliocentric velocity at which the crossovers occur from an inverted to an anti-inverted ground state population. Observations indicate that the Despois et al. model is better at some crossing points, and the Schleicher et al. model is better at others (see Fig. 9 in Schleicher & A'Hearn 1988). We have adopted here the inversion curve of Despois et al.. We recall that the derived OH production rates are roughly inversely proportional to the assumed inversion value. The reader may wish to avoid using production rates measured at times when the absolute value of the inversion is too small.

The OH Λ-doublet acts as a weak maser, amplifying (or attenuating) according to its inversion (or anti-inversion) the continuum background at the wavelengths of the 18-cm lines. Most of the time, the background temperature $T_{\rm bg}$ is close to 3 K, but it may be significantly higher when a comet crosses the galactic plane or an occasional discrete radio source. We have evaluated $T_{\rm bg}$ from the Stockert continuum survey at 1420 MHz (Reich & Reich 1986) performed with a 25′ beam, available as computer files. The 1420 MHz intensities are converted to 1667 MHz assuming a 2.7 K cosmic contribution and a galactic contribution with a mean spectral index of −2.6.

Table 3. Haser model parameters used in former and present analyses to derive water production rates for OH observations

	standard	1986A [a]	Haser-equivalent [b] with quenching	Haser-equivalent [b] with quenching and trapezium
parent velocity [km s^{-1}]	—	—	0.8	from line shapes [c]
parent lifetime [s]	—	—	8.5×10^4	8.5×10^4
parent scale length [km]	80 000	60 000	—	—
daughter velocity [km s^{-1}]	1.5	1.4	0.95	0.95
daughter lifetime [s]	4×10^5	10^5	1.1×10^5	1.1×10^5
quenching	none	none	[2]	[2]
used by	[1]	[3] [4] this work	[5] this work	[5] [6]

[a] The OH observers agreed upon this set of parameters at the time of the *International Halley Watch*. Note that Schloerb et al. (1987) give, for 1986A, vectorial model parameters which, when converted into Haser-equivalent parameters, are similar to those listed here.

[b] The parent and daughter *Haser-equivalent* scale lengths are computed from the lifetimes and velocities according to the formulas of Combi & Delsemme (1980).

[c] Derived from the fit of a trapezium to the line shape, according to Bockelée-Morvan et al. (1990a).

References: [1]: Despois et al. (1981); [2]: Gérard (1990); [3]: Gérard et al. (1988, 1989); [4]: Schloerb et al. (1987); [5]: Bockelée-Morvan et al. (1994); [6]: Bockelée-Morvan et al. (1990a).

Unfortunately, similar data south of $-19°$ declination are not yet available as computer files; the default value $T_{\rm bg}$ = 3.0 K is then assumed.

The inversion of the OH Λ-doublet may be quenched by collisions with ions and electrons. Neglecting this effect leads to an underestimation of the OH production rate, which explains the large discrepancies between UV and radio OH production rates obtained in the past. OH quenching was modelled by Despois et al. (1981), Schloerb (1988), Gérard (1990) and by Budzien (1992); see also recent studies by Gérard et al. (1998), Colom et al. (1999) and Schloerb et al. (1999). We have adopted the model of Gérard (1990) for which the radius r_q of the quenching region scales as:

$$r_q \propto r\, Q[\mathrm{OH}]^{\frac{1}{2}}. \quad (1)$$

r_q = 65 000 km has been determined for r = 1.38 AU and Q[OH] = 9.4×10^{28} s^{-1} from the observations of comet Halley. It should be noted, however, that the theory of OH quenching is still poorly constrained by the observations. r_q and Q[OH] were derived through an iterative process. In some cases (especially when the quenching zone is larger than the telescope beam), this process did not correctly converge.

The space distribution of the OH radical is described by a Haser-equivalent model (Combi & Delsemme 1980). The water and OH-radical lifetimes are set to 8.5×10^4 and 1.1×10^5 s, respectively (Table 3). We have not tried to include the effects of solar variability: they are discussed by Cochran & Schleicher (1993) and Budzien et al. (1994). The water expansion velocity $v_{\rm exp}$ is known to depend upon the heliocentric distance and the gas production rate. As shown by Bockelée-Morvan et al. (1990a), it can be derived from the OH line shapes when they are observed with a good signal-to-noise ratio. For determining the production rates or their upper limits in weak comets, we assumed this velocity to be $v_{\rm exp}$ = 0.8 km s^{-1}. The ejection velocity of the OH radical following water photodissociation was assumed to be 0.95 km s^{-1} (Crovisier 1989; Bockelée-Morvan et al. 1990a).

Choosing the best parameters for deriving Q[OH] is a difficult task. The user of XCOM can specify her/his preferred parameters. In order to derive automatically a uniform set of results, we have chosen in the present work to analyse and present the data with two sets of parameters: those described above (column 4 of Table 3), and *1986A* (column 2 of Table 3), which were parameters used at the time of the *International Halley Watch*. The latter set is particularly useful when the iterative process to evaluate the quenching radius does not properly converge. Of course, the resulting Q[OH] may differ from those we published elsewhere from the same observations.

For comets with reasonably small Q[OH] (typically $< 10^{-28}$ s^{-1}) not too close to the Earth or to the Sun (typically $\Delta, r > 1$ AU), the correction for quenching is not important. For such comets, $v_{\rm exp}$ is also close to 0.8 km s^{-1}. In this case, the three last models of Table 3 lead to similar production rates. For other comets, neglecting quenching could lead to significantly underestimated production rates.

The water expansion velocity, uniformly set to $v_{\rm exp}$ = 0.8 km s^{-1} in the present analysis, also leads to underestimated production rates for those comets which have higher velocities. Retrieving $v_{\rm exp}$ from line shapes (last model of Table 3), following Bockelée-Morvan et al. 1990a) requires spectra with high signal-to-noise ratios and is not appropriate to the automatic analysis we are presenting here. In extreme cases (1P/Halley and C/1995 O1 (Hale-Bopp) close to perihelion), $v_{\rm exp}$ could be as high as 2 km s^{-1}. In such cases, Q[OH] could be underestimated by about a factor of two, or even more taking into account the non-linearity of the correction for quenching.

Table 4. Maximum production rates determined for each comet in the Nançay data base, compared with production rates from ground-based visible OH and Lyman α.

comet			Nançay[d)]		other observations		
a)	b)	c)	max Q[OH] [10^{28} s^{-1}]	r [AU]	max Q[OH] [10^{28} s^{-1}]	r [AU]	
1982 I	1980b	C/1980 E1 Bowell	< 8.0	4.93			
1982 IV	1982a	26P/Grigg-Skjellerup	< 1.5	1.10	0.04	1.12	e)
1982 VI	1982g	C/1982 M1 Austin	9.4	0.76			
1982 VII	1982e	6P/d'Arrest	≈ 0.3	1.40	0.36	1.41	e)
1982 VIII	1982f	67P/Churyumov-Gerasimenko	≈ 0.9	1.35	0.35	1.41	e)
1984 IV	1983n	27P/Crommelin	≈ 1.1	0.76	1.0	0.71	e)
1984 XIII	1984i	C/1984 N1 Austin	25.4	0.51			
1985 XIII	1984e	21P/Giacobini-Zinner	6.0	1.04	3.2	1.12	e)
1985 XVII	1985l	C/1985 R1 Hartley-Good	2.5	0.76	2.0	0.89	e)
1985 XIX	1985m	C/1985 T1 Thiele	3.9	1.33	1.5	1.41	e)
1986 III	1982i	1P/1982 U1 Halley	108.6	0.71	35.	0.71	e)
1987 II	1986n	C/1986 V1 Sorrells	8.5	1.79	7.6	1.78	e)
1987 III	1987c	C/1987 B1 Nishikawa-Takamizawa-Tago	11.3	0.90	3.8	1.12	e)
1987 VII	1986l	C/1986 P1 Wilson	19.6	1.35			
1987 XXIX	1987s	C/1987 P1 Bradfield	9.5	0.93	3.9	1.12	e)
1988 I	1987d$_1$	C/1987 W1 Ichimura	12.9 ?	0.26			
1988 V	1988a	C/1988 A1 Liller	10.7	0.86	4.2	1.12	e)
1988 XV	1988j	C/1988 P1 Machholz	< 0.8	0.81			
1989 X	1989o	23P/1989 N1 Brorsen-Metcalf	23.5	0.53			
1989 XIX	1989r	C/1989 Q1 Okazaki-Levy-Rudenko	7.6	0.65			
1989 XXII	1989a$_1$	C/1989 W1 Aarseth-Brewington	20.7	0.58			
1990 V	1989c$_1$	C/1989 X1 Austin	44.4	0.38			
1990 XX	1990c	C/1990 K1 Levy	20.6	1.06			
1992 III	1991g$_1$	C/1991 Y1 Zanotta-Brewington	1.3	0.75			
1992 VII	1992b	C/1992 B1 Bradfield	< 1.3	0.58			
1992 VIII	1991h$_1$	C/1991 X2 Mueller	< 2.4	0.43			
1992 XIX	1991a$_1$	C/1991 T2 Shoemaker-Levy	2.9	1.11	1.5	0.89	e)
1992 XXVIII	1992t	109P/1992 S2 Swift-Tuttle	54.2	0.97	25.	0.89	e)
1993 III	1992x	24P/Schaumasse	1.0	1.28			
1994 V		2P/Encke	≈ 1.3	0.50			
1994 IX	1993p	C/1993 Q1 Mueller	4.9	0.99			
1994 XI	1993v	C/1993 Y1 McNaught-Russell	4.4	0.94			
1994 XV	1992r	8P/Tuttle	≈ 3.2	1.03			
1994 XXVI	1994o	141P/1994 P1 Machholz 2	≈ 1.3	0.76			
1994 XXX	1994l	19P/Borrelly	2.8	1.43			
		15P/Finlay (1995)	< 2.5	1.08			
		C/1995 Q1 Bradfield	17.5 ?	0.46			
		73P/Schwassmann-Wachmann 3 (1995)	22.2	0.95			
		122P/1995 S1 de Vico (1995)	61.0	0.68			
		45P/Honda-Mrkos-Pajdušáková (1996)	≈ 1.5	0.55	0.5	0.85	f)
		C/1996 B2 Hyakutake	20.3	0.70	56.	0.54	f)
		22P/Kopff (1996)	2.9	1.68			
		C/1996 Q1 Tabur	4.2	0.99	4.2	0.92	f)
		C/1995 O1 Hale-Bopp	463.3	0.92	1020.	0.91	f)
		46P/Wirtanen (1997)	< 1.5	1.12	1.5	1.08	f)
		81P/Wild 2 (1997)	≈ 0.8	1.74			
		2P/Encke (1997)	< 4.6	0.39	0.9	0.81	f)
		C/1998 J1 SOHO	30.3	0.87	71.	0.32	f)
		C/1998 P1 Williams	≈ 8.1	1.19			
		21P/Giacobini-Zinner (1998)	5.1	1.05			
		C/1998 U5 LINEAR	≈ 1.4	1.26			
		C/1999 H1 Lee	13.9	0.85			
		C/1999 N2 Lynn	6.4	0.77			

a) old-style definitive designation; b) old-style provisional designation; c) new-style designation (with year of perihelion for recent short-period comets); d) using parameters of column 4 in Table 3, see text; e) from visible observations of OH (A'Hearn et al. 1995); f) from Lyman α observations (Mäkinen et al. 2001a).

In extreme cases where the comet is highly productive like C/1995 O1 (Hale-Bopp) or came very close to the Earth like C/1996 B2 (Hyakutake), retrieving Q[OH] from observations aimed at the comet centre position, which are dominated by the quenched region, may be very difficult or even impossible. Help could come, however, from the analysis of observations made at offset positions. Such analyses are not presented here, and the reader is referred to our specific studies of comets Hyakutake and Hale-Bopp (Gérard et al. 1998; Colom et al. 1999).

How do our radio OH production rates compare with those obtained by other means? Systematic observations of the water (or OH) production rates have been achieved for an important number of comets: from ground-based observations of the A–X band of OH (A'Hearn et al. 1995); from space observations of the same band by *IUE* (for which no homogeneous analysis has yet been published); from Lyman α observations with *SOHO/SWAN* (Mäkinen et al. 2001a).

Table 4 lists the highest OH production rates determined for each comet in our data base (using parameters of column 4 of Table 3). For comparison, the Table reports Q[OH] derived from the ground-based spectrophotometric observations of A'Hearn et al. (1995), and $Q[H_2O]$ from the Lyman α observations of *SOHO/SWAN* (Mäkinen et al. 2001a), when such data has been published for a comparable heliocentric distance. The production rates from the ground-based visible observations of OH are systematically weaker, by a factor of 2 to 3, than those from Nançay. This can be attributed to the choice of the Haser-model parameters adopted by A'Hearn et al. (1995) (they assumed a parent scale length of 24 000 km, much shorter than our value). There is a more sound agreement with the production rates from the Lyman α data set. It is beyond the scope of the present paper to present a more detailed comparison of these various production rate determinations, which would involve a case-by-case study of the time evolution of each comet.

4. Comets observed between 1973 and 1981

Table 1 gives the list of all comets observed at Nançay up to 1999.

Observations made in 1973–1981 are not described here. There are only partly incorporated in the data base. Most of them were reported in Biraud et al. (1974), Despois (1978), Despois et al. (1981), Bockelée-Morvan et al. (1981), and Bockelée-Morvan (1982). Some representative spectra are also reproduced in Arpigny et al. (1999). Further information concerning these comets may be obtained on request.

5. Comets observed between 1982 and 1999

The rationale for cometary observations at Nançay evolved with time. In 1982, using for the first time a new receiver with a versatile backend, we tried to observe almost every "possible" object: five comets were observed, but only Austin 1982 VI yielded high quality spectra warranting meaningful scientific analyses. In the following years, we tried to optimize the scientific return of the observations by focusing our choice on bright comets, or on comets for which an observing campaign was set up. With some exceptions, the observations were scheduled only at the moments when the excitation of the OH radical was favourable.

The detailed log of all the observations made in 1982–1999 is given in tables available electronically. There is one entry per daily observation of a given comet. At the end of the set of observations of a given comet we also give the parameters of the spectra integrated over selected periods. Selections of the most representative spectra, for individual day observations or averages of several days as listed in the tables, are also available electronically.

As an example, we show here the log table and the figures for comet 22P/Kopff (Table 5 and Fig. 1).

The table columns are organized as follows:

- Date of the observation (`date`) (or range of dates for integrations).
- Geocentric distance (`delta`).
- Heliocentric distance (`r`).
- Heliocentric radial velocity (`rdot`).
- Theoretical inversion of the OH maser (`inv`) according to Despois et al. (1981).
- Theoretical inversion of the OH maser (`inv`) according to Schleicher & A'Hearn (1988).
- Background brightness temperature (`Tbg`) evaluated as explained in Sect. 3.
- The line area and its rms error (`area`), evaluated from -2.25 to 2.25 km s^{-1}.
- The line maximum intensity and its rms error (`S`).
- The line central velocity and its rms error (`Vo`).
- The line width at half maximum and its rms error (`dVo`). These three last items result from a Gaussian fit to the spectrum and are only listed when the signal-to-noise ratio of the line is larger than 3.
- The OH production rate and its rms error (or its 3–σ upper limit) (`Q[OH]`), using the *Haser-equivalent* model with quenching (Table 3, column 3) and the Despois et al. maser inversion. Null values are listed when the iterative algorithm to evaluate the quenching does not converge.
- The OH production rate and its rms error (or its 3–σ upper limit) (`Q[OH]`), using the *1986A* model (Table 3, column 2).
- The reference of the figure (`Fig.`) where the spectrum is shown.

When observations at offset positions were made, they are listed in a separate table in which the offsets (`offRA` and `offDec`) are listed instead of production rates.

Unless otherwise specified, the spectra shown in the figures are sums of the left- and right-handed circular polarizations and of the 1667 and 1665 MHz components, normalized to the 1667 MHz intensity (assuming the LTE ratio 1665:1667 = 5:9).

Table 5. Detailed log of the observations of comet 22P/Kopff and results for integrations over selected periods of time (from Tables A.42a and A.42b). A comprehensive data set for all comets is available electronically.

NANCAY 22P/Kopff

date	delta AU	r AU	rdot km/s	inv	inv	Tbg K	area mJy.km/s	S mJy	Vo km/s	dVo km/s	Q[OH] E28s-1	Q[OH] E28s-1	Fig.
960409-960412	1.13	1.78	-7.6	-0.31	-0.37	4.9	-85 12	-34 5	-0.03 0.18	2.34 0.45	2.5 0.4	2.6 0.4	A42.a
960419-960425	1.01	1.73	-6.8	-0.30	-0.36	10.2	-180 10	-94 5	-0.12 0.05	1.87 0.13	2.3 0.1	2.5 0.1	A42.a
960427-960430	0.94	1.71	-6.4	-0.29	-0.34	11.4	-296 11	-122 5	-0.22 0.05	2.16 0.11	2.9 0.1	3.2 0.1	A42.a
960501-960508	0.88	1.68	-5.9	-0.27	-0.33	5.3	-114 8	-60 3	-0.14 0.06	1.95 0.15	2.9 0.2	3.1 0.2	A42.a
960510-960515	0.81	1.66	-5.2	-0.25	-0.30	4.5	-92 11	-44 5	-0.22 0.11	1.94 0.28	2.7 0.3	2.7 0.3	A42.a
960516-960523	0.76	1.64	-4.6	-0.23	-0.27	4.3	-62 9	-38 4	-0.30 0.09	1.52 0.23	2.0 0.3	2.0 0.3	A42.a

NANCAY 22P/Kopff

date	delta AU	r AU	rdot km/s	inv	inv	Tbg K	area mJy.km/s	S mJy	Vo km/s	dVo km/s	Q[OH] E28s-1	Q[OH] E28s-1	Fig.
96/04/ 9.19	1.15	1.78	-7.7	-0.31	-0.37	4.9	-90 25	-48 15	0.75 0.25	0.85 0.59	1.3 0.4	1.3 0.4	A42.b
96/04/10.19	1.14	1.78	-7.6	-0.31	-0.37	4.9	-67 24				< 2.1	< 2.2	A42.b
96/04/11.18	1.13	1.78	-7.5	-0.31	-0.37	4.8	-87 24	-42 12	-0.20 0.29	2.06 0.72	2.7 0.7	2.8 0.8	A42.b
96/04/12.18	1.11	1.77	-7.5	-0.31	-0.37	4.8	-96 26	-48 12	-0.14 0.31	1.95 0.77	2.8 0.8	3.0 0.8	A42.b
96/04/13.18	1.10	1.77	-7.4	-0.31	-0.37	5.0	6 30				< 2.4	< 2.6	A42.b
96/04/14.18	1.09	1.76	-7.4	-0.31	-0.37	5.2	-12 24				< 2.0	< 2.0	A42.b
96/04/19.17	1.04	1.74	-7.0	-0.31	-0.37	7.1	-150 26	-71 11	-0.87 0.19	2.55 0.48	3.3 0.6	3.7 0.7	A42.c
96/04/20.17	1.03	1.74	-7.0	-0.31	-0.36	7.7	-137 27	-66 11	0.02 0.17	1.98 0.41	2.3 0.5	2.5 0.5	A42.c
96/04/21.17	1.01	1.73	-6.9	-0.30	-0.36	8.4	-139 22	-60 11	-0.05 0.19	2.23 0.48	2.1 0.3	2.3 0.4	A42.c
96/04/22.17	1.00	1.73	-6.8	-0.30	-0.36	9.6	-115 24	-106 14	0.02 0.09	1.29 0.23	2.0 0.4	2.1 0.4	A42.c
96/04/23.17	0.99	1.73	-6.8	-0.30	-0.36	11.6	-307 22	-146 12	-0.14 0.08	1.98 0.20	3.1 0.2	3.5 0.3	A42.c
96/04/24.17	0.98	1.72	-6.7	-0.30	-0.35	12.8	-132 41	-121 20	0.60 0.18	2.01 0.44	2.7 0.8	2.7 0.8	A42.c
96/04/25.16	0.97	1.72	-6.6	-0.30	-0.35	17.5	-292 32	-147 17	-0.36 0.11	1.87 0.27	2.1 0.2	2.2 0.2	A42.d
96/04/26.16	0.96	1.71	-6.5	-0.29	-0.35	26.0	-4138 353	-1919 91	-2.44 0.12	7.11 0.39	0.0 0.0	0.0 0.0	A42.d
96/04/27.16	0.95	1.71	-6.5	-0.29	-0.35	21.1	-538 27	-214 12	-0.11 0.06	2.23 0.16	2.8 0.1	3.2 0.2	A42.d
96/04/28.16	0.94	1.71	-6.4	-0.29	-0.34	10.4	-234 23	-94 10	-0.16 0.12	2.32 0.29	2.6 0.3	2.9 0.3	A42.d
96/04/29.16	0.93	1.70	-6.3	-0.29	-0.34	6.5	-214 26	-81 11	-0.51 0.15	2.23 0.37	3.4 0.4	3.9 0.5	A42.d
96/04/30.16	0.92	1.70	-6.2	-0.29	-0.34	6.4	-176 23	-98 12	-0.31 0.11	1.78 0.27	3.4 0.4	3.8 0.5	A42.d
96/05/ 1.15	0.91	1.70	-6.2	-0.28	-0.34	6.1	-179 26	-75 12	-0.38 0.15	1.94 0.38	3.0 0.4	3.3 0.5	A42.e
96/05/ 2.15	0.90	1.69	-6.1	-0.28	-0.33	5.9	-132 25	-71 13	-0.07 0.18	1.85 0.44	2.9 0.6	3.1 0.6	A42.e
96/05/ 3.15	0.89	1.69	-6.0	-0.28	-0.33	5.6	73 35				< 2.3	< 2.5	A42.e
96/05/ 4.15	0.89	1.69	-5.9	-0.28	-0.33	5.3	-144 22	-82 11	0.07 0.12	1.76 0.29	3.4 0.5	3.7 0.6	A42.e
96/05/ 5.15	0.88	1.68	-5.8	-0.27	-0.32	5.1	-156 25	-72 11	0.14 0.20	2.35 0.49	4.2 0.7	4.6 0.7	A42.e
96/05/ 6.15	0.87	1.68	-5.8	-0.27	-0.32	4.9	-162 27	-61 10	-0.16 0.20	2.60 0.50	4.2 0.7	4.5 0.8	A42.e
96/05/ 7.14	0.86	1.68	-5.7	-0.27	-0.32	4.8	-83 24	-59 11	-0.53 0.18	1.27 0.45	2.1 0.6	2.2 0.6	A42.f
96/05/ 8.14	0.85	1.67	-5.6	-0.27	-0.31	4.6	-109 25	-60 14	0.07 0.20	1.89 0.49	3.3 0.7	3.4 0.8	A42.f
96/05/10.14	0.83	1.67	-5.4	-0.26	-0.31	4.5	-97 30	-67 15	-0.08 0.17	1.27 0.42	2.6 0.8	2.6 0.8	A42.f
96/05/11.14	0.82	1.66	-5.3	-0.26	-0.30	4.5	-173 31	-62 14	-0.09 0.23	2.22 0.56	4.3 0.8	4.3 0.8	A42.f
96/05/12.14	0.82	1.66	-5.3	-0.25	-0.30	4.5	-50 22				< 2.0	< 2.0	A42.f
96/05/13.13	0.81	1.66	-5.2	-0.25	-0.30	4.4	-97 22	-37 10	-0.42 0.28	2.20 0.70	2.6 0.6	2.6 0.6	A42.f
96/05/14.13	0.80	1.65	-5.1	-0.25	-0.29	4.4	-84 22	-31 9	0.10 0.39	2.97 0.99	3.0 0.8	3.0 0.8	A42.g
96/05/15.13	0.79	1.65	-5.0	-0.24	-0.29	4.4	-74 43				< 4.0	< 3.9	A42.g
96/05/16.13	0.78	1.65	-4.9	-0.24	-0.28	4.4	-87 29	-54 19	0.09 0.25	0.99 0.61	1.8 0.6	1.7 0.6	A42.g
96/05/17.13	0.78	1.65	-4.8	-0.24	-0.28	4.3	-82 22	-42 10	-0.25 0.23	2.32 0.57	3.4 0.9	3.2 0.9	A42.g
96/05/18.12	0.77	1.64	-4.7	-0.23	-0.27	4.3	-126 38	-37 15	-0.31 0.51	2.75 1.28	3.6 1.1	3.4 1.0	A42.g
96/05/19.12	0.76	1.64	-4.6	-0.23	-0.27	4.3	-56 24				< 2.4	< 2.3	A42.g
96/05/20.12	0.75	1.64	-4.5	-0.23	-0.26	4.3	-81 22	-51 15	-0.55 0.19	0.89 0.46	1.7 0.5	1.5 0.4	A42.h
96/05/21.12	0.75	1.64	-4.4	-0.22	-0.26	4.3	0 32				< 2.9	< 3.1	A42.h
96/05/22.12	0.74	1.63	-4.3	-0.22	-0.25	4.2	-20 26				< 2.3	< 2.6	A42.h
96/05/23.11	0.73	1.63	-4.3	-0.21	-0.25	4.2	-47 20				< 2.0	< 2.0	A42.h

The individual observations of each comet are discussed separately in Appendix A.

6. Statistics

From 1973 to 1999, we have observed 60 different comets at Nançay (not counting multiple returns). 40 were clearly detected, and 12 marginally detected. Table 6 lists the distribution of these detections among different families of

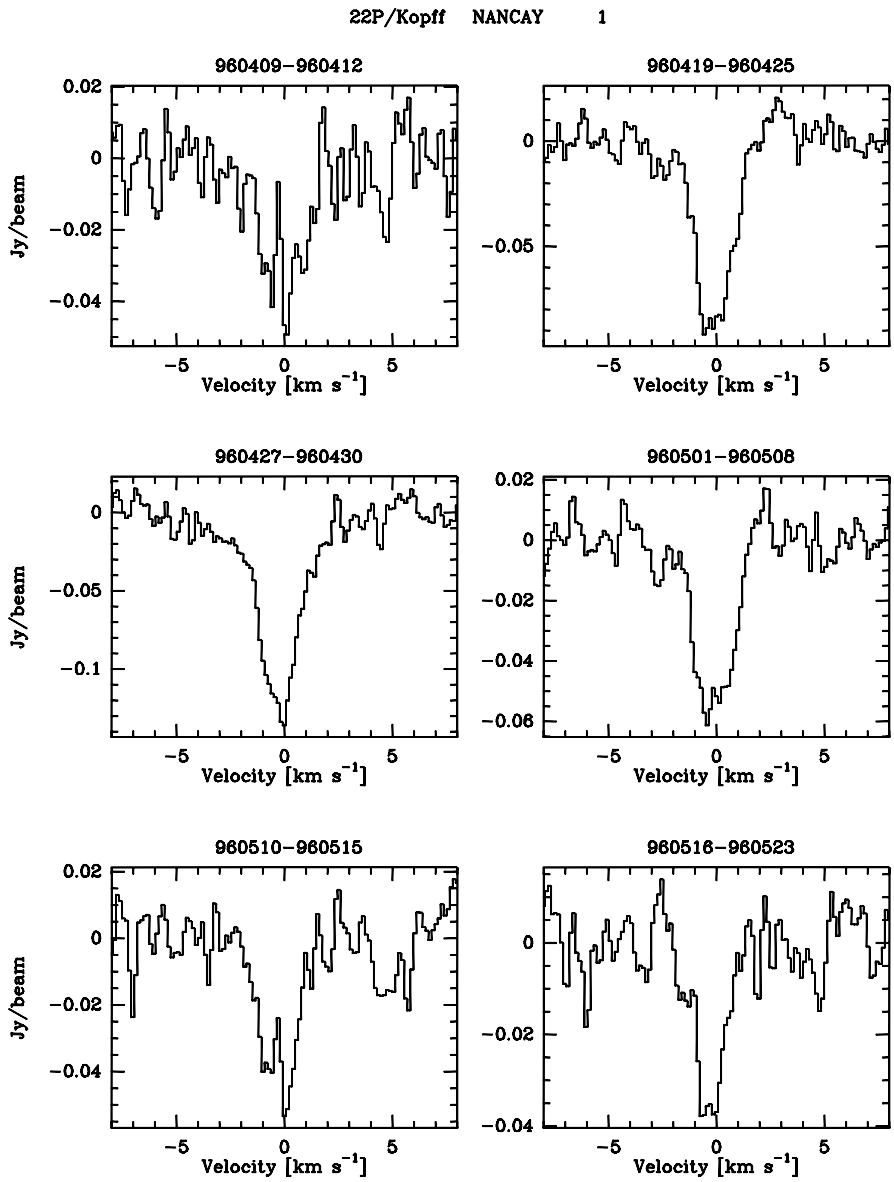

Fig. 1. Selection of representative spectra: comet 22P/Kopff (from Fig. A.42a). The spectra are integrated over selected periods of time, as given in Table 5. A comprehensive data set for all comets is available electronically.

Table 6. Comets observed at Nançay from 1973 to 1999: statistics of detections.

comet type	clear detection	marginal detection	not detected	total
long-period comets				
dynamically new	6	0	2	8
others	25	4	2	31
short-period comets				
Halley-type	4	2	0	6
Jupiter-family	5	6	4	15
total	40	12	8	60

comets, as listed in Table 1. Among long-period comets ($P > 200$ years), we have distinguished dynamically new comets (with semi major axis $a > 20\,000$ years) from others (with smaller a, or for which a could not be precisely determined). Among short-period comets, we have separated Jupiter-family ($P < 20$ years, small inclination) and Halley-type ($20 < P < 200$ years, random inclination) comets.

The upper limit that can be achieved on Q[OH] depends on r, Δ and the inversion i of the OH maser. For observations spread over one week (7×1 hour integration), the 3–σ upper limit on the line area is ≈ 0.030 K km s^{-1}. This corresponds to an upper limit Q[OH]

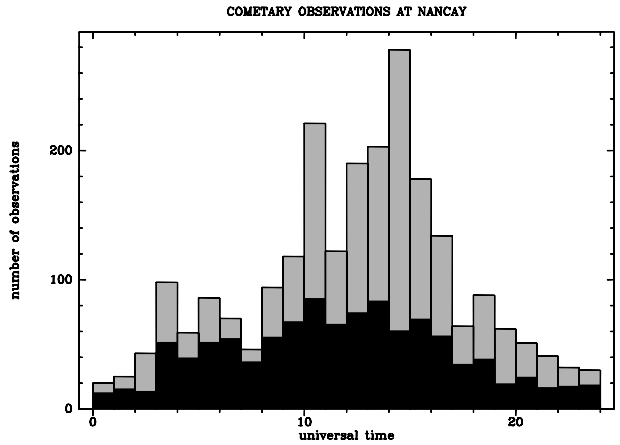

Fig. 4. Distribution of the observations as a function of universal time

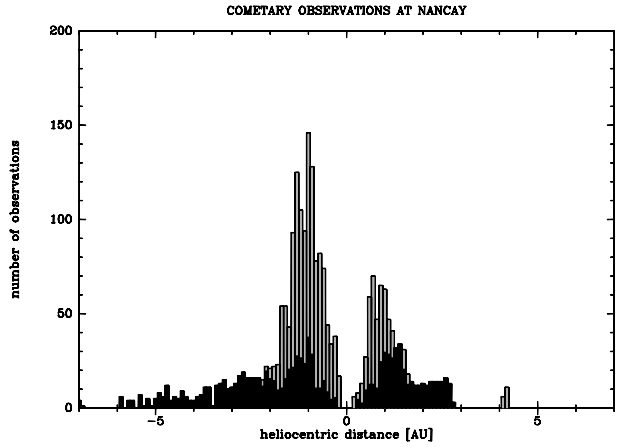

Fig. 5. Distribution of the observations as a function of heliocentric distance (negative: pre-perihelion; positive: post-perihelion)

Fig. 2. Histograms of the number of comets with Q[OH] observed larger than a given value. Three histograms are superimposed: short-period comets (black), long-period comets (grey) and full sample (white).

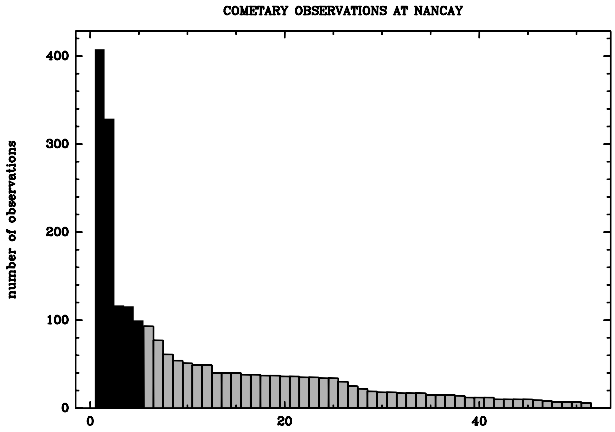

Fig. 3. Histogram of the number of observations per comet. The abscissa is a ranking number in order of number of observations. In Figs 3 to 7, the black part of the histograms refer to the five most-observed comets

$< 1.3 \times 10^{28}$ s^{-1} for a comet at $r = \Delta = 1$ AU with $i = 0.3$. Few comets, with better observing conditions, were detected with Q[OH] $< 10^{28}$ s^{-1}.

Fig. 2 shows the distribution of comets with Q[OH] larger than a given value (Q being the strongest OH production rate obtained during the scheduled observations of the comet, as listed in Table 4). There is an average of one comet per year observed with Q[OH] $> 10^{29}$ s^{-1}. We believe that we have not missed any comet at this production rate level, in the sky domain accessible to Nançay. Some comets, however, may have reached higher Q[OH] than those we observed, because radio observations of OH close to perihelion or at small heliocentric distances are more difficult (unfavourable OH maser inversion, higher quenching, smaller OH lifetime). Comets with small ($< 3 \times 10^{28}$ s^{-1}) Q[OH] are grossly under represented, because of the detection limit discussed above, and because observations of such weak comets were less frequently scheduled.

Figs 3–7 show some other aspects of the distribution of the Nançay observations. No discrimination has been made between observations with or without detection. Figure 3 is the histogram of the number of daily observations per comet. Five comets with 100 or more observations were the object of a peculiarly long campaign of observation and represent 45% of all observations. They are 1P/Halley, C/1995 O1 (Hale-Bopp), 21P/Giacobini-Zinner (1985 return), C/1986 P1 (Wilson) and C/1989 X1 (Austin), in order of decreasing number of observations. In Figs 3, 4, 5 and 7, these well-studied comets are shown

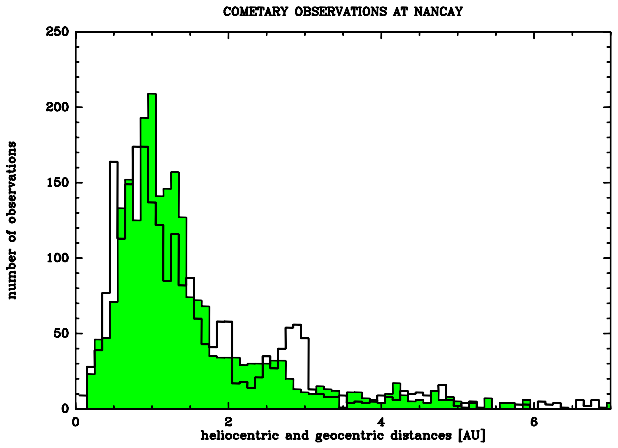

Fig. 6. Distribution of the observations as a function of heliocentric (in grey) and geocentric (plain thick line) distances

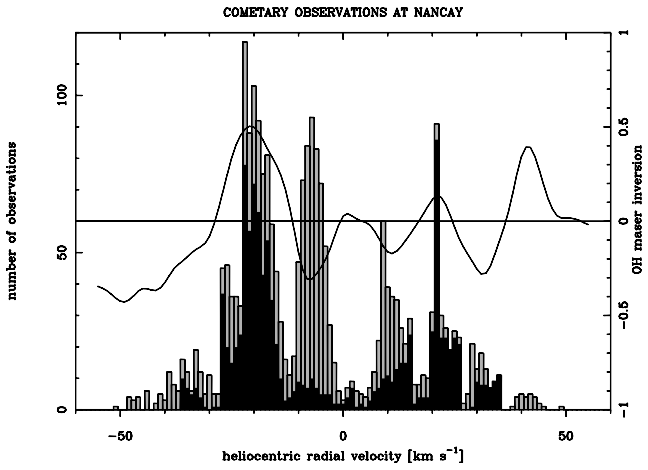

Fig. 7. Distribution of the observations as a function of heliocentric radial velocity. The OH maser inversion (from Despois et al. 1981) is also plotted

as black histograms, superimposed over grey histograms for the full sample.

Figure 4 is the histogram of the observations as a function of UT time. At Nançay, civil time is UT+8^m. The distribution shows that day-time observations are more numerous by a significant factor (1718 observations between 6.0 and 18.0 UT, to be compared to only 635 in the other UT hours). This is because observations were preferentially made when the comets are the most productive, which is when they are close to the Sun and therefore at small solar elongation. Why the distribution actually peaks in the afternoon is not understood. No significant trend is found in the distribution as a function of sideral time.

Figure 5 is the distribution of the heliocentric distances at which observations were made. More observations were made pre-perihelion rather than post-perihelion; the explanation is discussed with Fig. 7. Observations at more than ≈ 2 AU were only attempted in the brightest comets, among the five well-studied objects (except for comet Bowell (1982 I), which was observed – and undetected – at ≈ 4 AU post-perihelion).

Figure 6 shows together the distributions of heliocentric and geocentric distances of the observations (irrespective of the pre- or post-perihelion situation). We see that observations were generally made at smaller geocentric than heliocentric distances. This is still a consequence of our aim to make observations in the best observing conditions.

Figure 7 shows the distribution of the heliocentric radial velocities of the observations. This obviously uneven distribution can be easily understood: the excitation of the cometary OH maser strongly depends upon the heliocentric radial velocity and the signal is expected, in first approximation, to be proportional to the maser inversion. As a consequence, the observations were preferentially planned at the moments of strong inversions. The theoretical maser inversion is also plotted in the figure to show this correlation. Only for bright comets were observations made at the moment of weak inversion, to investigate other possible excitation mechanisms. On the average, the inversion is weaker post-perihelion (positive heliocentric velocities) compared to pre-perihelion. Accordingly, post-perihelion observations are less numerous.

7. Conclusion and prospects

We have attempted to present a most complete and comprehensive view of all the valuable OH cometary data taken at Nançay since 1973. The scientific exploitation of the data base is quite incomplete and it is hoped that the present paper will stir up new ideas and collaborations.

Clearly, some studies are lagging because the physics of OH cometary masers is not fully understood (e.g., the quenching mechanism and the non-thermal excitation of the OH transitions). This is also the case of the relation between the anisotropic outgassing and the non-gravitational forces, the average cometary magnetic field and its relation with the solar magnetic field structure. It is also true that the interest of cometary researchers has strongly shifted to millimetre wavelengths where many fundamental microwave lines have been discovered.

The Nançay radio telescope has undergone a major upgrade which started in 1995 and ended in 2000 (van Driel et al. 1996). The old Hoghorn feeds were replaced by a double Gregorian wide-band system with corrugated horns and sensitivity improved by a factor of 2.2. Furthermore, the horns can be rotated by $\pm 90°$ and provide full polarization capability. Thus, if the OH cometary maser is linearly polarized with an expected minimum along the comet–Sun direction (Mies 1976), the position angle of the orthogonal polarizations can be set in this direction[4]. A new autocorrelator has also been constructed

[4] However, the Larmor frequency of OH due to the weak magnetic field in the coma is much higher than the UV excitation rate of this radical. The polarization geometry could thus be dominated by the magnetic field rather than the Sun direction.

which provides for cometary observations 8 banks of 1024 channels in 195 kHz (190 Hz channel separation, corresponding to 0.035 km s^{-1}, or 0.07 km s^{-1} after Hanning smoothing). As in the past, a frequency-switching mode is used and subsequent folding results in a gain of a factor of 1.4. It is now possible to observe simultaneously the four OH transitions at 1665 and 1667 MHz (main lines) and 1612 and 1721 MHz (satellite lines) in both left- and right-hand circular polarizations, to detect possible Zeeman shifts and departures from the LTE line intensity ratios.

The new system has been successfully used already since July 2000 to detect four comets in 2000, namely C/1999 S4 (LINEAR) in early July 2000, before its disintegration (Bockelée-Morvan et al. 2001), C/1999 T1 (McNaught-Hartley) in November–December 2000, 73/P Schwassmann-Wachmann 3, and C/2000 W1 (Utsunomiya-Jones) in December 2000. These new observations will described in future publications.

With an increased sensitivity by a factor 2.2, one can either start observing "usual" comets at larger heliocentric distances or detect intrinsically fainter objects, or perform a more continuous monitoring of these objects. Alternately, one may wish to study the long- and short-term variations of the OH production rate associated with the outbursts, break-up of the cometary nuclei and correlate them with the production rates variations of other species and/or with the visual magnitude. Whatever the future strategy, the new system should allow to handle several cometary observations daily much more easily than in the past.

Acknowledgements. This paper is dedicated to the memory of Odile Franquelin and Gabriel Bourgois, who died during the course of this work.

Thanks are due to other observers in the early days of this programme (F. Biraud, I. Kazès, D. Despois and N. Hallet) for their help and to other members or visitors of the *groupe comètes* at Meudon (L. Jorda, N. Biver and H. Rauer) for their support.

The observations at Nançay would not have been possible without the help and support of the operators and of the technical staff of the radio telescope. These observations blindly rely on cometary ephemeris; we are very grateful to those who provided timely astrometric positions and orbital elements (B. Marsden and D. Green at the Central Bureau for Astronomical Telegrams, D. Yeomans at the Jet Propulsion Laboratory, and P. Rocher at the Bureau des longitudes).

The Nançay Radio Observatory is the Unité scientifique de Nançay of the Observatoire de Paris, associated as Unité de service et de recherche (USR) No B704 to the French Centre national de la recherche scientifique (CNRS). The Nançay Observatory also gratefully acknowledges the financial support of the Conseil régional of the Région Centre in France.

Appendix A: Comments on individual comets

Comments on individual comets are given below. Comets are listed following their perihelion dates as in Table 1. Individual passages (for 2P/Encke and 21P/Giacobini-Zinner) are listed separately.

A.1. Bowell 1982 I (1980b)

Table A.1 and Figs A.1a to A.1d.

This comet reached perihelion on 12 March 1982, at $q = 3.36$ AU from the Sun. Despite its large heliocentric distance, it was very active and presented occasional outbursts (A'Hearn et al. 1984). The UV bands of OH were detected as far as $r = 5.3$ AU from the Sun, which is unusual, and which was attributed to an important icy grain halo whose very large surface compensated the weak water sublimation at that heliocentric distance (A'Hearn et al. 1984). These observations and speculations motivated the observations at Nançay. They suffered from internal interferences in the receiving system. As a consequence, the 1665 MHz data are spoiled. The comet was not detected when observed again late after perihelion: this could be due to the disappearance of the icy grains after perihelion, as suggested by the decrease of the OH signal observed in the UV.

A.2. 26P/Grigg-Skjellerup 1982 IV (1982a)

Table A.2 and Figs A.2a to A.2c.

This short-period comet (period $P = 5.09$ years; perihelion on 14 April 1982 at $q = 0.99$ AU) was not detected at Nançay, despite the favourable distance to the Earth ($\Delta = 0.40$ AU). The integrated spectra reveal a marginal signal which is too broad to be of cometary origin. This comet was the target of the *Giotto Extended Mission* (GEM) in July 1992. The Nançay upper limit $Q[\mathrm{OH}] < 1.5 \times 10^{28}$ s^{-1} is consistent with the production rates derived from optical observations at that time.

A.3. Austin 1982 VI (1982g)

Table A.3 and Figs A.3a to A.3f.

The Nançay observations of this comet (perihelion on 24 August 1982 at $q = 0.65$ AU) extended from the end of June to the beginning of September 1982. In August, the comet approached the Earth to only $\Delta = 0.33$ AU. The June observations were made according to the elements of IAU Circ. No 3706. In July, the elements of IAU Circ. No 3708 were used, resulting in a position error increasing with time and amounting to about 1.5 beams in right ascension at the end of the month. Despite this offset, the comet was detected at the end of July. The ephemeris was updated in August with the elements of IAU Circ. No 3716 and a strong signal was detected at the correct position. At the end of August and in September, the position error, according to the IAU Circ. No 3721 elements, was only a small fraction of the beam.

In early August, the peak line intensity exceeded 0.25 K at 1667 MHz, which was then the strongest cometary signal ever recorded at Nançay (the signal was strengthened in part due to enhanced background radiation when the comet crossed the galactic plane on August 5). The high signal-to-noise ratios and the high spectral resolution of these data permitted an analysis of the line profiles to derive the kinematic properties of the coma (Bockelée-Morvan & Gérard, 1984; Bockelée-Morvan et al. 1990a), and a study of the Zeeman effect in order to estimate the magnetic field within the coma (Gérard, 1985). The satellite lines were also observed and marginally detected.

Schenewerk et al. (1986) reported unsuccessful observations of this comet at the *VLA* (Very Large Array).

A.4. 6P/d'Arrest 1982 VII (1982e)

Table A.4 and Figs A.4a to A.4g.

This short-period comet ($P = 6.38$ years; perihelion on 14 September 1982 at $q = 1.29$ AU) was observed at Nançay during most of July and August 1982 when it was at $\Delta \approx 0.7$ AU. The integration of all spectra shows a marginal detection of the comet at the 3–σ level. This comet is known to have a very asymmetric light curve, being brighter post-perihelion, where the water production rate could be as high as 3×10^{28} s^{-1} according to *IUE* observations (Festou et al. 1992). The Nançay observations were made only pre-perihelion, the maser inversion being unfavourable post-perihelion.

The OH radio lines were observed in 6P/d'Arrest at its preceding return in July 1976, when it was at $\Delta = 0.2$ AU, by Webber & Snyder (1977); these authors claimed detection of the 1665 MHz line in emission and of the 1667 MHz line in absorption, but the signal-to-noise ratio was poor.

A.5. 67P/Churyumov-Gerasimenko 1982 VIII (1982f)

Table A.5 and Figs A.5a to A.5d.

This short-period comet ($P = 6.61$ years; perihelion on 12 November 1982 at $q = 1.31$ AU) was observed on October 1982 taking advantage of a favourable geocentric distance ($\Delta \approx 0.50$ AU). Like for comet Bowell 1982 I, internal interferences in the receiving system ruined most of the observations and only part of the 1667 MHz spectra could be analysed. The integration of all spectra shows a marginal detection of the comet at the 3.5–σ level.

A.6. 27P/Crommelin 1984 IV (1983n)

Table A.6 and Figs A.6b to A.6g.

This weak comet ($P = 27.4$ years; perihelion on 10 February 1984 at $q = 0.73$A) was proposed as a "trial run comet" in order to prepare the international campaign of 1P/Halley's observations. This comet was hardly detectable.

The significant average spectra from the Nançay observations were published, together with observations made with the Effelsberg 100-m and Green Bank 43-m telescopes, by Bockelée-Morvan et al. (1985). They are also included in the International Halley Watch (IHW) archive (IHW Archive 1992). The comet was also observed unsuccessfully at Arecibo (Deich et al. 1985) and at the *VLA* (Schenewerk et al. 1986).

A.7. Austin 1984 XIII (1984i)

Table A.7 and Figs A.7a to A.7d.

The comet (perihelion on 12 August 1984 at only $q = 0.29$ AU) was clearly detected at Nançay as soon as the observations were possible (Gérard & Drouhin, 1984). At that moment, an outburst was obviously present, since the signal disappeared afterwards more rapidly than expected. See also Bockelée-Morvan et al. (1990a).

A.8. 21P/Giacobini-Zinner 1985 XIII (1984e)

Tables A.8a and A.8b and Figs A.8a to A.8v.

This comet was designated as a target for an international campaign of observation in order to provide a ground support for its fly-by by the *International Comet Explorer* (ICE) spacecraft on September 11, 1985. It reached perihelion on 5 September 1985 at $q = 1.03$ AU (coinciding with the closest approach at $\Delta = 0.47$ AU). The Nançay observations were published by Gérard et al. (1988). They are included in the IHW archive (IHW Archive 1992) as well as OH radio observations by several other groups which are not given in detail here. See also Bockelée-Morvan et al. (1990a).

A.9. Hartley-Good 1985 XVII (1985l)

Tables A.9a and A.9b and Figs A.9a to A.9r.

This comet (perihelion on 9 December 1985 at $q = 0.69$ AU) was observed daily from the end of September 1985 to mid-January 1986. It was detectable until the end of November. See Gérard et al. (1986) and Bockelée-Morvan et al. (1990a).

This comet was also observed at the Green Bank 43-m telescope (Tacconi-Garman et al. 1990).

A.10. Thiele 1985 XIX (1985m)

Tables A.10a and A.10b and Figs A.10a to A.10g.

This comet (perihelion on 19 December 1985 at $q = 1.32$ AU) was daily observed at Nançay from the end of October to mid-December. It was clearly detected on integrated spectra. See Gérard et al. (1986) and Bockelée-Morvan et al. (1990a).

This comet was also observed at the Green Bank 43-m telescope (Tacconi-Garman et al. 1990).

A.11. 1P/Halley 1986 III (1982i)

Tables A.11a to A.11c and Figs A.11a to A.11bz (including offset position spectra).

This comet (perihelion on 9 February 1986 at $q = 0.59$ AU) was the object of a well documented international observing campaign (*International Halley Watch* IHW) as a support to its space exploration. The Nançay observations of this comet were published by Gérard et al. (1989) and are included in the IHW archive (IHW Archive 1992). They are not discussed in detail here. See also Gérard et al. (1987), Colom & Gérard (1988), Gérard (1990) and Bockelée-Morvan et al. (1990a).

Many other radio observations of this comet were performed, like the OH excited lines, the microwave transitions of other molecules and the continuum (see Crovisier & Schloerb 1991 and IHW Archive 1992).

A.12. Sorrells 1987 II (1986n)

Table A.12 and Figs A.12a and A.12b.

This comet (perihelion on 9 March 1987 at $q = 1.72$ AU) was detected in January–February 1987. See also Bockelée-Morvan et al. (1990a).

A.13. Nishikawa-Takamizawa-Tago 1987 III (1987c)

Table A.13 and Figs A.13a and A.13b.

This comet (perihelion on 17 March 1987 at $q = 0.87$ AU) was observed and detected in early March. Like for the preceding one, the signal-to-noise ratio was not large enough to justify continuous and detailed observations.

A.14. Wilson 1987 VII (1986l)

Tables A.14a and A.14b and Figs A.14a to A.14w.

This comet was discovered in August 1986, well ahead of perihelion (20 April 1987, at $q = 1.20$ AU). It was observed at Nançay from the end of August 1986 until the end of June 1987. The comet was, as a rule, monitored every second day, except from 5 April to 15 May when it was under the declination range accessible to the telescope (which, unfortunately, was the period of closest approach to the Sun and to the Earth). At other times, the comet was observed daily: at the beginning of the observing period and around the moment of molecular millimetre observations with the *IRAM* (Institut de radioastronomie millimétrique) 30-m telescope (Crovisier et al. 1987; Crovisier et al. 1990).

The comet was detected right at the beginning of the observations, at the end of August 1986 when it was at $r = 2.8$ AU, as a weak and narrow line (Gérard 1987). The comet, which was detectable all along the observing period, is one of the comets best studied at large heliocentric distances, allowing us to study the kinematics of H_2O and OH at large heliocentric distances. The production rate increased significantly from October to November 1986 (Gérard et al. 1986) and high signal-to-noise spectra were secured. These observations represent, besides 1P/Halley's and C/1995 O1 (Hale-Bopp) observing campaigns, the most continuous and rewarding cometary project undertaken at Nançay. See also Bockelée-Morvan et al. (1990a).

This comet was also observed and detected at the Green Bank 43-m telescope (Tacconi-Garman et al. 1990) and at the *VLA* (Palmer et al. 1989).

A.15. Bradfield 1987 XXIX (1987s)

Tables A.15a and A.15b and Figs A.15a to A.15g.

This relatively bright comet (perihelion on 7 November 1987 at $q = 0.87$ AU) was observed daily during October and the second half of November 1987. It was detected during the whole period. See also Bockelée-Morvan et al. (1990a).

A.16. Ichimura 1988 I (1987d_1)

Table A.16 and Figs A.16a and A.16b.

This comet was included in Nançay observing program because of its small perihelion distance ($q = 0.20$ AU on 10 January 1988) in order to test the quenching models versus heliocentric distance. It was tracked from orbital elements given in IAU Circ. No 4505. It was found afterwards (MPC 12710) that the tracked position was offset by 0.4 to 1.0′ in right ascension relative to the comet nucleus, which has negligible influence on the observations. In the integration of the 4–6 January spectra, the comet was detected at the 4.5–σ level as a relatively broad line. This increased line width is likely due to the small heliocentric distance: with an average value of $r = 0.26$ AU, the heliocentric distance of the observation is the smallest at which the OH radio lines were detected.

A.17. Liller 1988 V (1988a)

Table A.17 and Figs A.17a and A.17b.

This comet (perihelion on 31 March 1988 at $q = 0.85$ AU) was observed at Nançay to complement the OH observations scheduled at the *VLA* (de Pater et al. 1991).). The comet was tracked from parabolic orbital elements given in MPC 12587. Subsequent improved elliptic elements (MPC 13459) revealed that on March 22, the tracking was offset by 1.3′ in right ascension, −5.5′ in declination and 0.27 km s^{-1} in velocity[5]. The resulting line area is underestimated by a factor of 1.35. The comet was nevertheless clearly detected in the integration of the 6 spectra.

A.18. Machholz 1988 XV (1988j)

Table A.18 and Figs A.18a to A.18d.

This comet was discovered at the beginning of August 1988; a simple extrapolation of its light curve predicted that this object could be very interesting in mid September, because of its small perihelion distance (only 0.15 AU on 17 September 1988; IAU Circ. No 4637, 4644). Millimetre observations of HCN could be scheduled on short notice at *IRAM* 30-m telescope (Crovisier et al. 1990). Unfortunately, the Nançay radio telescope was closed for maintenance in September; it was nevertheless possible to squeeze observations on September 12–13. We used orbital elements from Green (1988, *personal communication*) almost identical to those given in MPC 13591.

Comet Machholz did not behave as expected. Its brightness ceased to increase at the beginning of September. It was then lost optically because of its small solar elongation. Deep searches between 25 and 35 days after perihelion were negative (IAU Circ. No 4669). It is thus one of those comets which disappears near perihelion. The moment at which the comet actually ceased outgassing is unknown. The Nançay observation gives an upper limit to its activity around perihelion.

This comet was observed at 18 cm at the *VLA* (de Pater et al. 1991), also unsuccessfully.

A.19. 23P/Brorsen-Metcalf 1989 X (1989o)

Table A.19a and A.19b and Figs A.19a to A.19m.

This comet is of the Halley type with a period of 70.6 years. It was already observed at its two last passages and had a favourable return in 1989 (perihelion on 11 September 1989 at $q = 0.48$ AU; closest approach to Earth: $\Delta = 0.62$ AU at the beginning of August). It appeared to be the best opportunity among short-period comets until the end of the century, besides 1P/Halley and 109P/Swift-Tuttle (whose return was still speculative at that time). Therefore, several observations on large instruments could be scheduled and an observing campaign could be coordinated. The Nançay radio telescope participated in this campaign by observing this comet almost daily from the beginning of August until the end of October. Until September 30, the observations were made with orbital elements of IAU Circ. No 4805. Later, osculating elements for October 1 provided by Yeomans (*personal communication*, August 11, 1989) were used.

The comet was detected at the beginning of the observations; at that moment, the signal was weak due to the low inversion of the OH Λ-doublet. Spectra with high signal-to-noise ratios were obtained at the end of August–beginning of September. In October, the comet could only be detected after long integration times, showing that the gas production

[5] All reported offsets are *tracked parameter − real parameter*.

rate was smaller post-perihelion than pre-perihelion (Bockelée-Morvan et al. 1990b).

Like the following comets, this comet was observed at a time of high solar activity. As a consequence, the water life time is expected to be shorter (by a factor which may be as high as two), and the quenching by collisions with ions may be higher (due to the higher ionization rate by solar UV), compared to periods of quiet Sun.

This comet was also observed (but not detected) at the Green Bank 43-m telescope (Schloerb 1989, *personal communication*, as quoted by Crovisier 1992).

A.20. Okazaki-Levy-Rudenko 1989 XIX (1989r)

Tables A.20a and A.20b and Figs A.20a to A.20k.

This comet (perihelion on 11 November 1989 at $q = 0.64$ AU; closest approach to Earth at $\Delta = 0.52$ AU at the beginning of December) was detected after the first few days of observation in October. It was observed until December 2, when it was below the southern declination limit at Nançay. Observations of 3–7 October were made with the orbital elements of MPC 15053; the error in right ascension was $-0.7'$. All subsequent observations were made with orbital elements of MPC 15215; the maximum error was $0.4'$ in right ascension and $1.5'$ in declination at the end of November (with respect to final elements of MPC 15520).

On October 13.54 we observed serendipitously the occultation of a background point radio source by this comet (Bockelée-Morvan et al. 1989; Crovisier et al. 1992): the line has increased in intensity and decreased in width, compared to the average line observed before and after the occultation of the source B2 1426+295, as expected from the hypothesis of the OH maser amplification of the background. From mid-October until the end of November, the OH production rate derived from the radio observations is nearly constant, despite the varying distance to the Sun (Bockelée-Morvan et al. 1990b).

This comet was also observed at the *VLA* (de Pater et al. 1989, *personal communication*) and with the Green Bank 43-m telescope (Schloerb 1989, *personal communication*, as quoted by Crovisier 1992).

A.21. Aarseth-Brewington 1989 XXII (1989a1)

Table A.21 and Figs A.21a to A.21d.

This comet (perihelion on 27 December 1989 at $q = 0.30$ AU) was observed from December 8 until December 30 when it went below the declination range accessible to the Nançay telescope. Observations were made with orbital elements of MPC 15520; the position errors (RA, δ), which were negligible at the beginning of the observations, were ($0.4'$, $0.7'$) on Dec. 25, ($1.0'$, $0.6'$) on Dec. 30 with respect to confirmed elements of MPC 15672.

The comet was easily detected until Dec. 17. Afterwards, the signal was harder to extract, due to the rapidly changing OH inversion near perihelion, and presumably of the large collisional quenching at this small solar distance (Bockelée-Morvan et al. 1990b).

A.22. Austin 1990 V (1989c_1)

Tables A.22a and A.22b and Figs A.22a to A.22t.

This comet passed perihelion on 9 April 1990 at $q = 0.35$ AU and made a close approach to Earth at $\Delta = 0.24$ AU on 25 May 1990. The observations are described by Bockelée-Morvan et al. (1990b). Successful millimetre observations of this comet were also conducted at *IRAM*.

A.23. Levy 1990 XX (1990c)

Tables A.23a to A.23c and Figs A.23a to A.23v (including offset position spectra).

This comet passed perihelion on 24 October 1990 at $q = 0.94$ AU. The observations are described by Bockelée-Morvan et al. (1992) and Gérard et al. (1993). The strong OH lines allowed to detect the satellite lines and the Zeeman effect. It was the first comet in which a reversal of the projected magnetic field was observed. The evolution of the magnetic field seems to be correlated with $\sin\theta \sin\phi$, θ being the Sun–comet–Earth angle and ϕ the heliomagnetic latitude of the comet (Gérard et al. 1993).

Successful millimetre observations of this comet were also conducted at *IRAM*. An analysis of the OH radio line shapes was made by Xie (1994).

A.24. Zanotta-Brewington 1992 III (1991g_1)

Table A.24 and Figs A.24a to A.24d.

This comet passed perihelion on 31 January 1992 at $q = 0.64$ AU. It was detected in mid-January. Post-perihelion observations were not possible because of the low declination of the comet. See also Bockelée-Morvan et al. (1994).

A.25. Bradfield 1992 VII (1992b)

Table A.25 and Figs A.25a and A.25b.

This comet passed perihelion on 19 March 1992 at $q = 0.50$ AU. OH could not be detected pre-perihelion. It was not recovered post-perihelion from visible observations (IAU Circ. No 5469). See also Bockelée-Morvan et al. (1994).

A.26. Mueller 1992 VIII (1991h_1)

Table A.26 and Figs A.26a to A.26c.

This comet passed perihelion on 21 March 1992 at only $q = 0.20$ AU. Like the preceding one, it could not be detected pre-perihelion at Nançay (the feature on the integrated spectrum is due to interferences) and was not recovered post-perihelion from visible and infrared observations (IAU Circ. No 5482 and 5496). See also Bockelée-Morvan et al. (1994).

A.27. Shoemaker-Levy 1992 XIX (1991a_1)

Tables A.27a and A.27b and Figs A.27a to A.27h.

This comet passed perihelion on 23 August at $q = 0.83$ AU. The observations are described by Bockelée-Morvan et al. (1994).

A.28. 109P/Swift-Tuttle 1992 XXVIII (1992t)

Tables A.28a to A.28c and Figs A.28a to A.28m (including offset position spectra).

The observations of this Halley-type comet ($P = 135$ years, perihelion on 12 December 1992 at $q = 0.96$ AU) are described by Colom et al. (1992) and Bockelée-Morvan et al. (1994). Strong asymmetries were observed in the OH lines as well as in the molecular millimetre and submillimetre lines observed at *IRAM* and with the *JCMT* (James Clerk Maxwell Telescope) (Bockelée-Morvan et al. 1994; Despois et al. 1996), which could be the counterpart of the strong dust jets observed in the visible.

A.29. 24P/Schaumasse 1993 III (1992x)

Tables A.29a and A.29b and Figs A.29a to A.29f.

This comet, which passed perihelion on 3 March 1993 at $q = 1.20$ AU, was formerly a possible target for the *ROSETTA* mission. It was detected at Nançay in January–February 1993. These observations are described by Bockelée-Morvan et al. (1994).

A.30. 2P/Encke 1994 V

Tables A.30a and A.30b and Figs A.30a to A.30g.

Despite a long integration time and a rather favourable return ($\Delta \approx 0.63$ AU), the comet was – at most – only marginally detected. Thus our observations of the same comet in 1980 (Bockelée-Morvan et al. 1981), favoured by the crossing of the galactic plane, could not be improved.

A.31. Mueller 1994 IX (1993p)

Tables A.31a and A.31b and Figs A.31a to A.31h.

This comet reached perihelion on 26 March 1994 at $q = 0.97$ AU. It was observed and detected at Nançay during two runs in February and March. The tracking was based upon the elements of MPC 22663 and 23106, the position error being at most $0.2'$ in RA in February.

A.32. McNaught-Russell 1994 XI (1993v)

Tables A.32a and A.32b and Figs A.32a to A.32f.

This comet reached perihelion on 31 March 1994 at $q = 0.87$ AU from the Sun and was then relatively close to the Earth ($\Delta \approx 0.6$ AU). The observations were made using elements of MPC 23107 and 23224, which did not significantly differed, for the positions at the moment of the observations, from the confirmed elements of MPC 23322. The comet was detected during three observing runs in March and April at Nançay.

A.33. 8P/Tuttle 1994 XV (1992r)

Table A.33 and Figs A.33a to A.33c.

8P/Tuttle was observed at Nançay just before its perihelion on 25 June 1994 (MPC 20775) at $q = 1.00$ AU. Despite its large geocentric distance, but benefiting from an enhanced background continuum, this comet was marginally detected with a production rate ($\approx 3 \times 10^{28}$ s^{-1}) in agreement with that determined optically at its preceding passage in 1980 (A'Hearn et al. 1995).

A.34. 141P/Machholz 2 1994 XXVI (1994o)

Table A.34 and Figs A.34a and A.34b.

141P/Machholz 2 passed perihelion on September 18, 1994, at $q = 0.75$ AU. Soon after its discovery, this comet was found to have multiple nuclear components (IAU Circ. No 6066, 6070 and 6071). The Nançay observations, made on September 1994 just before perihelion, were aimed at the main component. We used elements of MPC 23858, which at the time of the observations differed by less than $0.3'$ in RA from the confirmed elements of MPC 23956. We only obtained a marginal detection with an intensity lower than that expected from its visual magnitude. We infer that the brightness of the comet in the visible was enhanced by the release of dust following the disruption of its nucleus.

A.35. 19P/Borrelly 1994 XXX (1994l)

Tables A.35a and A.35b and Figs A.35a to A.35j.

19P/Borrelly, which was the flyby target of the *Deep Space 1* mission on 22 September 2001, made a favourable return in 1994, staying at $\Delta \approx 0.65$ AU in November–December. It passed perihelion on November 1, 1994, at $q = 1.37$ AU. This comet was observed as part of a campaign which included radio observations at *IRAM* and at the *JCMT*, space observations with *IUE* and the *HST*, and several ground-based observations in the visible.

19P/Borrelly was detected at Nançay during the 5 September–11 October pre-perihelion period (Bockelée-Morvan et al. 1995), with a production rate of $\approx 2.5 \times 10^{28}$ s^{-1}, whereas the production rate expected at perihelion from previous observations is $\approx 5 \times 10^{28}$ s^{-1}. It could not be detected in a post-perihelion run in January 1995 (upper limit $< 2 \times 10^{28}$ s^{-1}), presumably because of unfavourable observing conditions (high declination and weaker maser inversion).

A.36. 15P/Finlay (1995 passage)

Table A.36 and Figs A.36a to A.36c.

15P/Finlay was one of the backup targets for the *ROSETTA* international mission. Its 1995 return (perihelion on 15 May 1995 at $q = 1.04$ AU) was not favourable, the comet being on the other side of the Sun, always at a small solar elongation and at $\Delta > 1.9$ AU from the Earth. Thus it could not be recovered before the Nançay observations, which were based on elements extrapolated from last passage astrometric positions (MPC 20122). Observed in April 1995, the comet was not detected, the upper limit on the gas production rate ($< 2.5 \times 10^{28}$ s^{-1}) being in agreement with the expected production rate from the visible magnitudes ($\approx 2 \times 10^{28}$ s^{-1}) according to Jorda et al. (1996).

A.37. C/1995 Q1 (Bradfield)

Table A.37 and Figs A.37a to A.37d.

This comet was discovered late, just before its perihelion passage (on August 31, 1995, at $q = 0.44$ AU). It was then as bright as $m_v = 5.5$. The first observations were made (until September 5) using orbital elements communicated by Marsden (*personal communication*), close to those published in IAU Circ. No 6208. Then, elements of MPC 25623 were used. The RA offset was $0.8'$ on 4 September. The OH lines

were detected at the 5–σ level around perihelion (August 24–September 5).

A.38. 73P/Schwassmann-Wachmann 3 (1995 passage)

Tables A.38a and A.38b and Figs A.38a to A.38h.

73P/Schwassmann-Wachmann 3 was formerly the nominal target of the *ROSETTA* international mission and was present in the list of backup targets. From the visual magnitudes observed at its preceding passages, the OH production rate of this comet was expected to be only of the order of 2×10^{28} s^{-1}. The comet was observed at Nançay from the beginning of September 1995, before its perihelion on 22 September at $q = 0.93$ AU. No signal was detected during the first days of observation. Unexpectedly, a signal appeared on September 8 and persisted on the following days, as long as the inversion was significant (Crovisier et al. 1995). The corresponding production rate is about 2×10^{29} s^{-1}, ten times larger than expected. This strongly suggests that the comet had an outburst. Following the announcement of this unexpected high production rate, visible observations revealed that the comet was indeed in a state of outburst with $m_v \approx 8.3$, i.e., a brightening of ~ 5 mag. (IAU Circ. No 6234). Images taken at a later time showed that the comet nucleus had split (IAU Circ. No 6274).

We benefited from the passage of the comet in front of the galactic centre region at the end of October 1995 to observe an enhanced signal due to the stronger background continuum. A full account of these observations is given by Crovisier et al. (1996a).

A.39. 122P/de Vico (1995 passage)

Table A.39 and Figs A.39a to A.39c.

This Halley-type comet ($P = 74.4$ years), which was considered as lost after its 1846 apparition, was recovered only three weeks before its perihelion (6 October 1995 at $q = 0.66$ AU). Observations could be organized at Nançay around perihelion, revealing a production rate exceeding 2×10^{29} s^{-1}.

A.40. 45P/Honda-Mrkos-Pajdušáková (1996 passage)

Tables A.40a and A.40b and Figs A.40a to A.40g.

This comet passed at only $\Delta = 0.17$ AU from the Earth on 6 February 1996 after its perihelion on 25 December 1995 at $q = 0.53$ AU. Millimetre and submillimetre observations were attempted at the *JCMT* at the moment of the closest approach. Only marginal detections could be obtained at Nançay.

A.41. C/1996 B2 (Hyakutake)

Tables A.41a and A.41b and Figs A.41a to A.41i.

C/1996 B2 (Hyakutake) made a very close approach to Earth at only $\Delta = 0.11$ AU on 25 March 1996 before its perihelion on 1 May 1996 at $q = 0.23$ AU, which made it an exceptionally bright comet at the end of March.

This comet was observed at Nançay since the first of March 1996. Rough mapping revealed stronger signal at offset positions, indicating the effect of quenching. The OH satellite lines could be detected, but only a marginal Zeeman effect could be observed. These observations were reported by Gérard et al. (1998). The spectra obtained at offset positions are not presently included in the data base.

The OH 18-cm lines were searched for, but not detected, at the *VLA* around perihelion time (de Pater, *personal communication*). It was the object of extensive millimetre and submillimetre observations.

A.42. 22P/Kopff (1996 passage)

Tables A.42a and A.42b and Figs A.42a to A.42h.

This Jupiter-family comet (perihelion on 2 July 1996 at $q = 1.58$ AU) was designated as a target for the *ISO* Central Program. It was observed pre-perihelion at Nançay using orbital elements provided by the Bureau des longitudes during most of April and May 1996. Despite its small OH production rate ($\approx 2.5 \times 10^{28}$ s^{-1}), it was easily detected since the beginning of the observations, benefiting from enhanced galactic continuum when it crossed the galactic plane (at $l = 14.5^\circ$ on 24 May). Galactic contamination was noted at that moment; it was especially strong on May 26 when the comet passed across the radio source M17.

The log of the observations of 22P/Kopff is given in Table 5 and representative spectra are shown in Fig. 1, as an example of the data which are only available electronically.

This comet was also observed at *IRAM*.

A.43. C/1996 Q1 (Tabur)

Table A.43 and Figs A.43a to A.43d.

C/1996 Q1 (Tabur) passed perihelion on 3 November 1996 at $q = 0.84$ AU. Its orbit similar to that of comet Liller 1988 V strongly suggests that both objects are fragments from the same parent body. It made a close approach to Earth in early October 1996 (0.42 AU) and was then very easily observable at Nançay with a production rate $\approx 5 \times 10^{28}$ s^{-1}. It could not be detected on 20–27 October, with a production rate upper limit 5 times smaller that observed at the beginning of October. Its visual brightness dropped similarly at the same moment. This comet may have had a fate similar to that of comet C/1999 S4 (LINEAR), whose nucleus was completely disrupted close to perihelion. This comet was also observed at *IRAM*.

A.44. C/1995 O1 (Hale-Bopp)

Tables A.44a to A.44c and Figs A.44a to A.44dn (including offset position spectra).

This comet was intrinsically very bright ($m_v \approx 10.5$) when it was detected in July 1995, at more than 7 AU from the Sun. This comet was about 100 times brighter than P/Halley at the same heliocentric distance. It passed perihelion on 1 April 1997, at $q = 0.91$ AU. An international campaign was organized for this comet, also designated as an exceptional target-of-opportunity comet for *ISO* observations.

A first try to detect OH at Nançay in this comet, on 4–9 August 1995 when it was at $r = 7$ AU, was negative (Biver et al. 1996). The upper limit is 2×10^{29} s^{-1} with the standard model. However, CO production rates of several 10^{28} s^{-1} were measured soon after at the *JCMT* (IAU Circ. No 6234) and at *IRAM* (IAU Circ. No 6236 and Biver et al. 1996). Periodic observations of this comet were made at the rate of about 8 days every month in order to detect the onset of water sublimation from its icy grains. The first OH detection at 18-cm was made

in mid-April 1996 (Crovisier et al. 1996b), just after its detection in the UV by the *HST* (IAU Circ. No 6376). The comet was then at 4.7 AU from the Sun: this is the farthest heliocentric distance at which 18-cm OH has been detected. More regular observations could be done afterwards, allowing a detailed monitoring of its OH production rate, to be compared with the monitoring of production rates of other molecules at other wavelengths, and especially those made at *IRAM*, *JCMT* and *CSO* (Caltech Submillimeter Observatory). This monitoring is reported in Biver et al. (1997, 1999a) and Colom et al. (1999).

The comet was observed until September 1997, when it escaped the declination range accessible to Nançay. For a large part of the time, it was close to the galactic plane (it even passed in front of the W 49 galactic source). As long as the signal was strong (from 10 October 1996 to 3 August 1997), offset observations were made in addition to centre observations in order to better determine the quenching conditions (see Colom et al. 1999).

Other radio OH observations of this comet are summarized by Despois (1999).

An attempt to observe the 9-cm lines of the CH radical at Nançay was made from 30 April to 20 May 1997. Neither the 3263 nor the 3335 MHz line of CH was detected down to a 3–σ level of 0.035 K km s^{-1}. The CH lines of a background source (L1534 of the Taurus molecular cloud complex), however, were detected at a velocity different from that of the comet, providing a check of the instrumentation. Detection of the 9-cm radio lines of CH in comet Kohoutek (1973 XII) was claimed by Black et al. (1974), but could not be confirmed (Rydbeck et al. 1974). These lines are Λ-doubling transitions within the $X^2\Pi$ rotational ground state of CH, similar to the 18-cm lines of OH. Their excitation should also be similar and governed by fluorescence of the A–X system in the violet: one would expect weakly masering lines, with inversion of the Λ-doublet depending upon the heliocentric velocity. The model has never been made, but even in case of maximum inversion, one would expect lines much weaker than the OH 18-cm lines because of the smaller column density of CH (the lifetime of CH is much shorter than that of OH).

A.45. 46P/Wirtanen (1997 passage)

Tables A.45a and A.45b and Figs A.45a to A.45h.

46P/Wirtanen is the target of the *ROSETTA* mission. It passed perihelion on 14 March 1997 at $q = 1.06$ AU. The observing conditions of the present return were highly unfavourable, the comet being at small solar elongation and at $\Delta > 1.5$ AU. The comet was observed at Nançay during two periods, pre- and post-perihelion, when the inversion of the OH maser is predicted to be high. The OH lines could not be detected. Since during these two periods, the observing conditions (distances to Sun and Earth, OH maser inversion) were practically constant, the spectra were averaged over each period of observation. We thus derived $Q[\mathrm{OH}] < 1.5 \times 10^{28}$ s^{-1} between beginning of February and beginning of March, $Q[\mathrm{OH}] < 2.4 \times 10^{28}$ s^{-1} between end of April and beginning of May (Crovisier et al. 2001).

From the light curves of previous returns, Jorda & Rickman (1995) and Rickman & Jorda (1998) evaluated the water production rate of 46P/Wirtanen to be 1.5–6$\times 10^{28}$ s^{-1} at perihelion. A'Hearn et al. (1995) measured $Q[\mathrm{OH}] \sim 1.1 \times 10^{28}$ s^{-1} close to the perihelion of the 1991 return; as discussed by Rickman & Jorda (1998), this evaluation might be an underestimate because of the use of inappropriate parameters in the Haser model describing the OH distribution.

During the 1997 return, optical observations could only be performed pre-perihelion due to unfavourable viewing conditions. Using the FOS instrument of the Hubble Space Telescope on 15 January (at $r = 1.3$ AU from the Sun) to measure the OH band in the UV, Stern et al. (1998) reported a water production rate $\sim 0.6 \times 10^{28}$ s^{-1}. From measurements of the Ly α line with the *SWAN* instrument aboard the *SOHO* spacecraft, Bertaux et al. (1999) estimated $Q[\mathrm{H_2O}] = 1.6 \pm 0.4 \times 10^{28}$ s^{-1} near perihelion. Farnham & Schleicher (1998) measured $Q[\mathrm{OH}] = 0.8 \times 10^{28}$ s^{-1} from narrow-band photometry at Lowell Observatory on 5 March ($r = 1.07$ AU).

The intercomparison of these results and of the Nançay limits is not direct because the production rates were not always derived with the same Haser model parameters for OH. However, the non-detections at Nançay appear to be consistent with the low production rates derived from the UV observations.

A.46. 81P/Wild 2 (1997 passage)

Tables A.46a and A.46b and Figs A.46a to A.46h.

81P/Wild 2 (the target of the *Stardust* mission) passed perihelion on 6 May 1997 at $q = 1.58$ AU. It was observed at Nançay almost daily from the end of January to the end of March. This corresponds to the period of best observing conditions. The observations of this comet were more sensitive than those of comet 46P/Wirtanen due to the closest distance of the comet to the Earth. The comet is detected from the average of all the observations (Crovisier et al. 2001). The line is relatively narrow, with a width comparable to those observed for comets with small gas production rates (Bockelée-Morvan et al. 1990a). The production rate is $Q[\mathrm{OH}] = 0.8 \pm 0.2 \times 10^{28}$ s^{-1} at an average distance $r_h = 1.74$ AU. With *SOHO*/*LASCO*, Mäkinen et al. (2001b) observed $Q[\mathrm{H_2O}] = 1.3 \times 10^{28}$ s^{-1} around perihelion, which compares well with our determination. Fink et al. (1999) also measured pre-perihelion production rates from the [OI] line which agree with ours.

A.47. 2P/Encke (1997 passage)

Table A.47 and Figs A.47a and A.47b.

2P/Encke was observed at its 1997 passage despite unfavourable conditions, as a programme proposed by M.C. Festou. It was not detected.

A.48. C/1998 J1 (SOHO)

Table A.48 and Figs A.48a and A.48b.

As a consequence of the work for the upgrading of the radio telescope, comets could only be observed for less than 40 minutes in 1998 and 1999 instead of one hour.

C/1998 J1 (SOHO) was one of the many comets discovered by the space coronagraph *LASCO* aboard *SOHO*. It passed perihelion on 8 May 1998 at $q = 0.15$ AU. Unlike most of the other *SOHO* comets, this comet was not a member of the Kreutz family and was sufficiently bright post-perihelion to justify radio observations. Unfortunately, the astrometric positions provided by *SOHO* suffered from systematic errors

and the first observations at Nançay were a failure. Only later observations made at the beginning of June on the basis of confirmed orbital elements from ground based observations (IAUC 6913) could be successful (Crovisier et al. 1998). They were made at the moment of an outburst noted by visual observers (IAUC 6926) and the production rate was as large as $\approx 3\times10^{29}$ s^{-1}. They had to be interrupted soon after when the comet passed below the declination limit of the radio telescope.

A.49. C/1998 P1 (Williams)

Table A.49 and Figs A.49a to A.49c.

C/1998 P1 (Williams) (perihelion on 17 October 1998 at $q = 1.15$ AU) was barely detected during a short pre-perihelion run. This comet was also observed at the *JCMT*.

A.50. 21P/Giacobini-Zinner (1998 passage)

Tables A.50a and A.50b and Figs A.50a to A.50e.

The 1998 return of 21P/Giacobini-Zinner was less favourable than the 1985 return (see Sect. 5.8). However, the comet crossed the galactic plane at the end of October, resulting in a significantly enhanced signal. Observations at Nançay were scheduled in coordination with other radio and infrared observations at *JCMT*, *CSO*, *IRAM* and *IRTF*. The OH production rate was found to be close to that of the preceding return.

A.51. C/1998 U5 (LINEAR)

Table A.51 and Figs A.51a to A.51c.

C/1998 U5 (LINEAR) (perihelion on 21 December 1998 at $q = 1.24$ AU) passed at $\Delta = 0.44$ AU on 16 November. Its brightness increased abruptly by ≈ 1.5 mag in mid-November. Observations began at Nançay on 24 November using orbital elements of MPC 32866, then the updated elements of MPEC 1998–W45. Only a marginal detection was obtained. This comet was also observed at the *CSO*.

A.52. C/1999 H1 (Lee)

Tables A.52a and A.52b and Figs A.52a to A.52m.

C/1999 H1(Lee) passed perihelion on 11 July 1999 at $q = 0.708$ AU. It was easily detected pre-perihelion with a production rate that culminated at 1.5×10^{29} s^{-1}, but could not be detected post-perihelion (Biver et al. 1999b). The observations are published together with the campaign of radio observations at other wavelengths (Biver et al. 2000).

A.53. C/1999 N2 (Lynn)

Table A.53 and Fig. A.53.

C/1999 N2 (Lynn) was discovered shortly before it passed perihelion (on 23 July 1999 at $q = 0.761$ AU). It was observed during four days pre-perihelion on short notice, and was just detected (production rate $\approx 6 \times 10^{28}$ s^{-1}).

References

A'Hearn, M.F., Millis, R.L., Schleicher, D.G., Osip, D.J., & Birch, P.V, 1995, Icarus 118, 223

A'Hearn, M.F., Schleicher, D.G., Feldman, P.D., Millis, R.L., & Thompson, D.T., 1984, AJ 89, 579

Arpigny, C., Dossin, F., Woszczyk, N., et al., 1999, Atlas of Cometary Spectra (Kluwer), in press

Bertaux, J.-L. Costa, J., Mäkinen, T., et al., 1999, Planet. Space Scie. 47, 725

Biraud, F., Bourgois, G., Crovisier, J., et al., 1974, A&A 34, 163

Biver, N., Bockelée-Morvan, D., Colom, P., et al., 1997, Scie 275, 1915

Biver, N., Bockelée-Morvan, D., Colom, P., et al., 1999a, Earth Moon Planets 78, 11

Biver, N., Bockelée-Morvan, D., Colom, P., et al., 1999b, IAU Circ. No 7203

Biver, N., Bockelée-Morvan, D., Crovisier, J., et al., 2000, AJ 120, 1554

Biver, N., Rauer, H., Despois, D., et al., 1996, Nature 380, 137

Black, J.H., Chaisson, E.J., Ball, J.A., Penfield, H., & Lilley, A.E., 1974, ApJ 191, L45

Bockelée-Morvan, D., 1982, Production, Cinématique et Asymétries de la Coma OH dans les Comètes C/Meier 1978 (XXI), C/Bradfield (1979 X), C/Meier (1980q), C/Bradfield (1980t) et Encke, thèse de 3e cycle, Université Paris VI.

Bockelée-Morvan, D., Biver, N., Colom, P., et al., 1995, Bull. Amer. Astron. Soc. 27, 1144

Bockelée-Morvan, D., Biver, N., Moreno, R., et al., 2001, Science 292, 1339

Bockelée-Morvan, D., Bourgois, G., Colom, P., et al., 1994, Planet. Space Scie. 42, 193

Bockelée-Morvan, D., Bourgois, G., Crovisier, J., & Gérard, E., 1989, IAU Circ. No 4882

Bockelée-Morvan, D., Colom, P., Crovisier, J., Gérard, E., & Bourgois, G., 1992, in Asteroids, Comets, Meteors 1991, Edts A.W. Harris & E. Bowell, 73

Bockelée-Morvan, D., Crovisier, J., & Gérard, E., 1990a, A&A 238, 382

Bockelée-Morvan, D., Crovisier, J., Gérard, E., & Bourgois, G,. 1990b, in Workshop on Observations of Recent Comets, Edts W.F. Huebner et al., 75

Bockelée-Morvan, D., Crovisier, J., Gérard, E., et al., 1985, AJ 90, 2586

Bockelée-Morvan, D., Crovisier, J., Gérard, E., & Kazès, I., 1981, Icarus 47, 464

Bockelée-Morvan, D., & Gérard, E., 1984, A&A 131, 111

Bockelée-Morvan, D., Padman, R., Davies, J.K., & Crovisier, J., 1994, Planet. Space Scie. 42, 655

Budzien, S.A., 1992, Physical and chemical processes of the inner coma observed in mid-ultraviolet cometary spectra, PhD dissertation, Johns Hopkins University

Budzien, S.A., Festou, M.C., & Feldman, P.D., 1994, Icarus 107, 164

Cochran, A.L., & Schleicher, D.G., 1993, Icarus 105, 235

Colom, P., Bockelée-Morvan, D., Bourgois, G., et al., 1992, IAU Circ. No 5643

Colom, P., & Gérard E,. 1988, A&A 204, 327

Colom, P., Gérard, E., & Crovisier, J., 1990, in Asteroids Comets Meteors III, edts C.-I. Lagerkvist et al., 293

Colom, P., Gérard, E., Crovisier, J., et al., 1999, Earth Moon Planets 78, 37

Combi, M.R., & Delsemme, A.H.,, 1980, ApJ 237, 633

Crovisier, J., 1989, A&A 213, 459

Crovisier, J., 1992, in Asteroids, Comets Meteors 1991, Edts A.W. Harris & E. Bowell, 137

Crovisier, J., Bockelée-Morvan, D., Colom, P., Gérard, E., & Biver, N. 1998, IAU Circ. No 6934
Crovisier, J., Biver, N., Bockelée-Morvan, D., et al., 1995, IAU Circ. No 6227
Crovisier, J., Biver, N., Bockelée-Morvan, D., et al., 2001, ESA SP-1165 (in press)
Crovisier, J., Bockelée-Morvan, D., Bourgois, G., & Gérard, E., 1992, A&A 253, 286
Crovisier, J., Bockelée-Morvan, D., Gérard, E., et al., 1996a, A&A 310, L17
Crovisier, J., Despois, D., Bockelée-Morvan, D., et al., 1990, A&A 234, 535
Crovisier, J., Despois, D., Bockelée-Morvan, D., & Gérard, E., 1987, IAU Circ. No 4411
Crovisier, J., Gérard, E., Colom, P., et al., 1996b. IAU Circ. No 6394
Crovisier, J., & Schloerb, F.P., 1991, in Comets in the Post-Halley Era, R.L. Newburn, M. Neugebauer & J. Rahe edts (Kluwer, Dordrecht), 149
Deich, W.T.S., Cordes, J.M., & Terzian, Y., 1985, AJ 90, 373
de Pater, I., Palmer, P., & Snyder L.E., 1991, in Comets in the Post-Halley Era, R.L. Newburn, M. Neugebauer & J. Rahe edts (Kluwer, Dordrecht), 175
Despois, D., 1978, Étude Radio Astronomique du Radical OH dans les Comètes, Thèse de 3^e cycle, Université Paris VI.
Despois, D., 1999, Earth Moon Planets 79, 103
Despois, D., Biver, N., Bockelée-Morvan, D., et al., 1996, Planet. Space Scie. 44, 529
Despois, D., Gérard, E., Crovisier, J., & Kazès, I., 1981, A&A 99, 320
Farnham, T., & Schleicher, D., 1998, A&A 335, L50
Feldman, P.D., 1999, Earth Moon Planets 79, 145
Festou, M.C., Feldman, P.D., & A'Hearn, M.F., 1992, in Asteroids, Comets Meteors 1991, Edts A.W. Harris & E. Bowell, 177
Fink, U., Hicks, M.P. & Fevig, R.A., 1999, Icarus 141, 331
Gérard, E., 1985, A&A 146, 1
Gérard, E,. 1987, in Workshop on Cometary Radio Astronomy, NRAO Workshop No 17, 91
Gérard, E., 1990, A&A 230, 489
Gérard, E., Bockelée-Morvan, D., Bourgois, G., Colom, P., & Crovisier, J., 1986, IAU Circ. No 4271
Gérard, E., Bockelée-Morvan, D., Bourgois, G., Colom, P., & Crovisier, J., 1987, A&A 187, 455
Gérard, E., Bockelée-Morvan, D., Bourgois, G., Colom, P., & Crovisier, J., 1988, A&AS 74, 485
Gérard, E., Bockelée-Morvan, D., Bourgois, G., Colom, P., & Crovisier, J., 1989, A&AS 77, 379
Gérard, E., Bockelée-Morvan, D., Colom, P., & Crovisier, J., 1993, in Astrophysical Masers, edts A.W. Clegg & J.E. Nedoluha, Lectures Notes in Physics 412 (Springer-Verlag), 468
Gérard, E., Crovisier, J., Colom, P., et al., 1998, Planet. Space Scie. 46, 569
Gérard, E., & Drouhin, J.P., 1984, IAU Circ. No 3967
IHW Archive, 1992
Jorda, L., 1995, Atmosphères cométaires: Interprétation des Observations dans le Visible et Comparaison avec les Observations Radio, thesis, Université Paris VII
Jorda, L., Crovisier, J., & Green, D.W.E., 1992, in Asteroids Comets Meteors 1991, edts A.W. Harris & E. Bowell, 285
Jorda, L., Crovisier, J., & Green, D.W.E., 1996, preprint
Jorda, L., & Rickman, H., 1995, Planet. Space Scie. 43, 575
Mäkinen, J.T.T., Bertaux, J.-L., Pulkkinen, T.I. et al., 2001b, A&A 368, 292
Mäkinen, J.T.T., Silén, J., Schmidt, W. et al., 2001b, Icarus 152, 268
Mies, F.H., 1974, ApJ 191, L145
Mies, F.H., 1976, in The Study of Comets, edts B. Donn, M. Mumma, W. Jackson, M. A'Hear, & R. Harrington, NASA SP-393, 843
Palmer, P., de Pater, I., & Snyder, L.R., 1989, AJ 97, 1791
Reich, P., & Reich, W., 1986, A&AS 63, 205
Rickman, H., & Jorda, L., 1998, Adv. Space Sci. 21(11), 1491
Rydbeck, O.E.H., Ellder, J., Ronnang, B., et al. 1974, Icarus 23, 595
Schenewerk, M.S., Palmer, P., Snyder, L.E., & de Pater, I., 1986, AJ 92, 166
Schleicher, D.G., & A'Hearn, M.F., 1988, ApJ 331, 1058
Schloerb, F.P., 1988, ApJ 332, 524
Schloerb, F.P., Claussen, M.J., & Tacconi-Garman, L., 1987, A&A 187, 469
Schloerb, F.P., Devries, C.H., Lovell, A.J., et al., 1999, Earth Moon Planets 78, 45
Stern, S.A., Parker, J.W., Festou, M.C., et al., 1998, A&A 335, L30
Tacconi-Garman, L.E., Schloerb, F.P., & Claussen, M.J., 1990, ApJ 364, 672
Turner, B., 1974, ApJ 189, L137
van Driel, W., Pezzani, J., & Gérard, E., 1996, in High Sensitivity Radio Astronomy, edts N. Jackson & R.J. Davis (Cambridge Univ. Press, Cambridge, UK), 229
Webber, J.C., & Snyder, L.E., 1977, ApJ 214, L45
Xie, X., 1994, Cometary Atmospheres: Monte Carlo Simulation and its Application to OH Radio Observations, PhD dissertation, University of Pensylvania